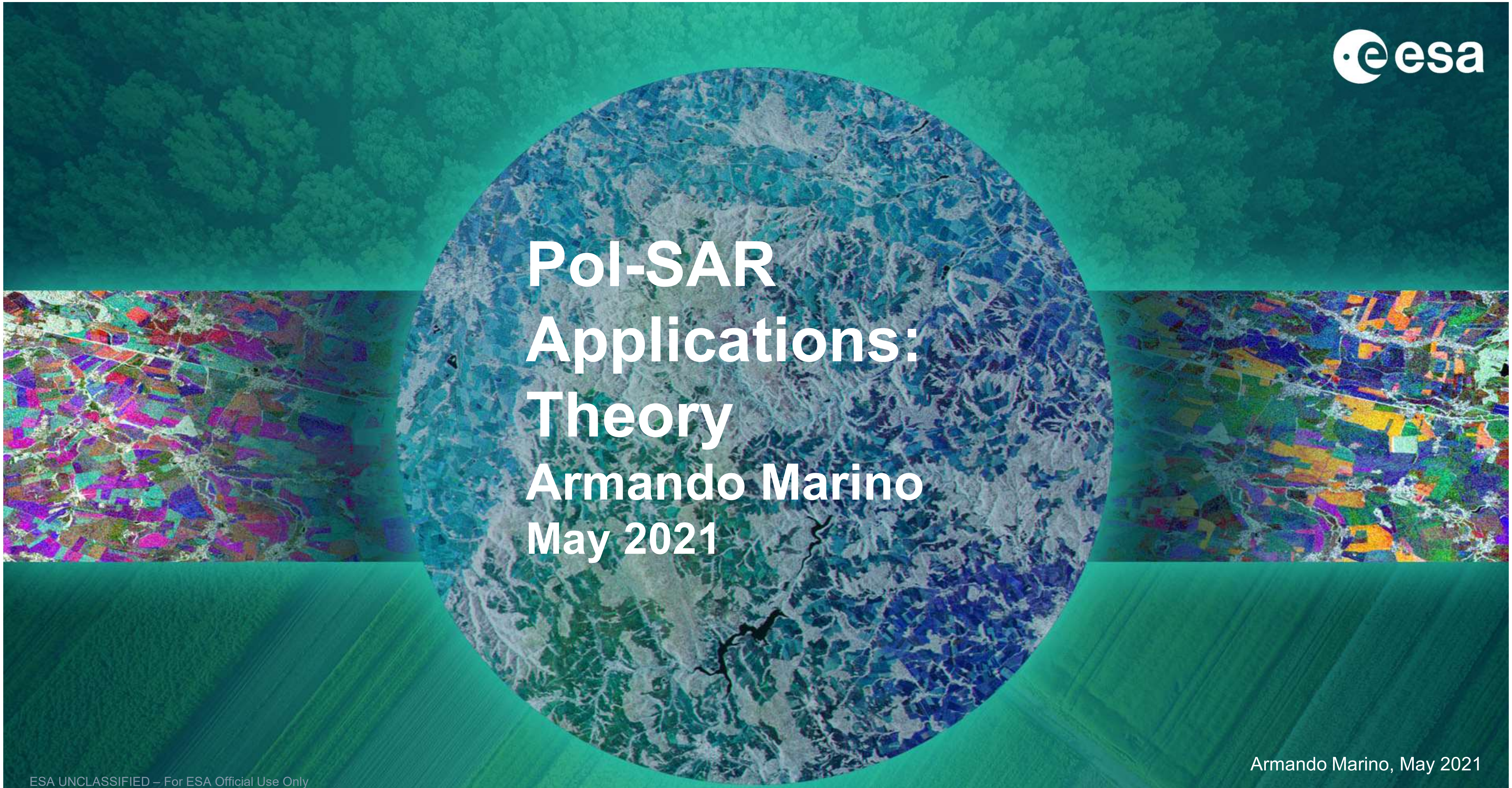

Pol-SAR Applications: Theory

Armando Marino

May 2021

UNIVERSITY of STIRLING

Senior Lecturer in Earth observation,
Biological and Environmental Sciences
University of Stirling
FK9 4LA | Stirling | UK
Earmando.marino@stir.ac.uk

© A. Marino 2021

PolSAR-App

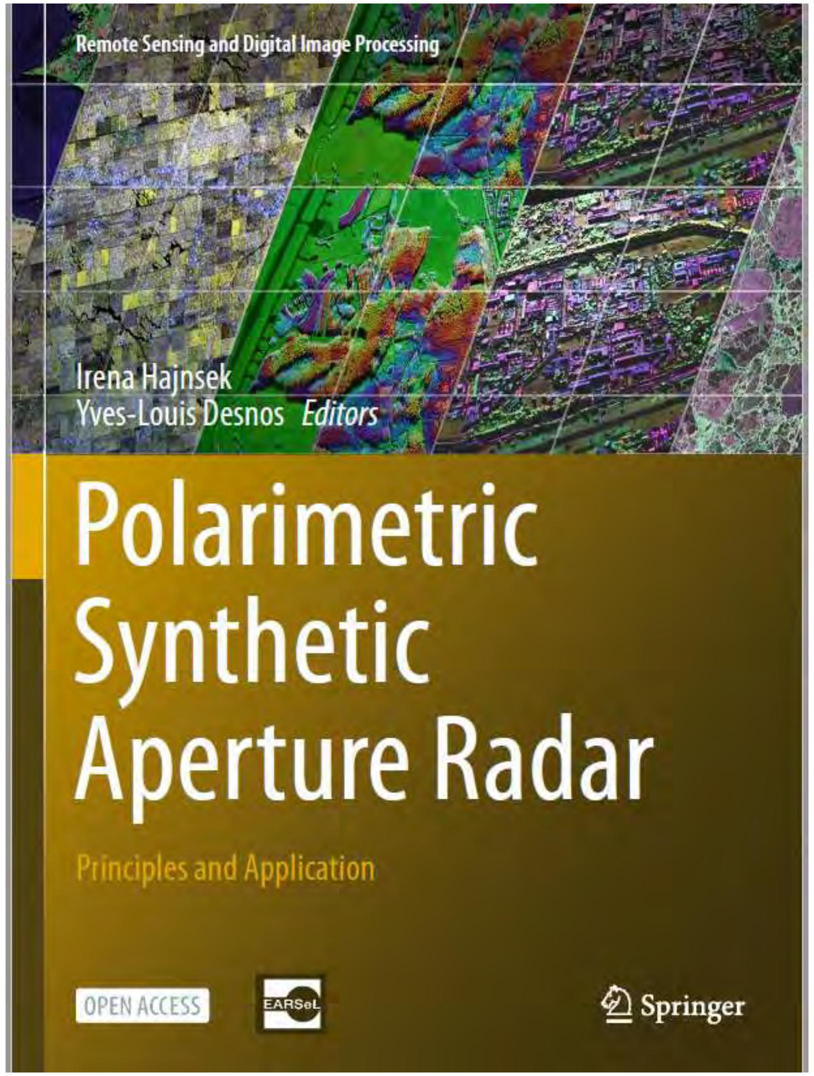

Remote Sensing and Digital Image Processing

Irena Hajnsek
Yves-Louis Desnos *Editors*

Polarimetric
Synthetic
Aperture Radar

Principles and Application

OPEN ACCESS

EARSeL

Springer

POLSAR-App in PolSARpro – Biomass Edition

ENTRY SCREEN

MAIN WINDOW

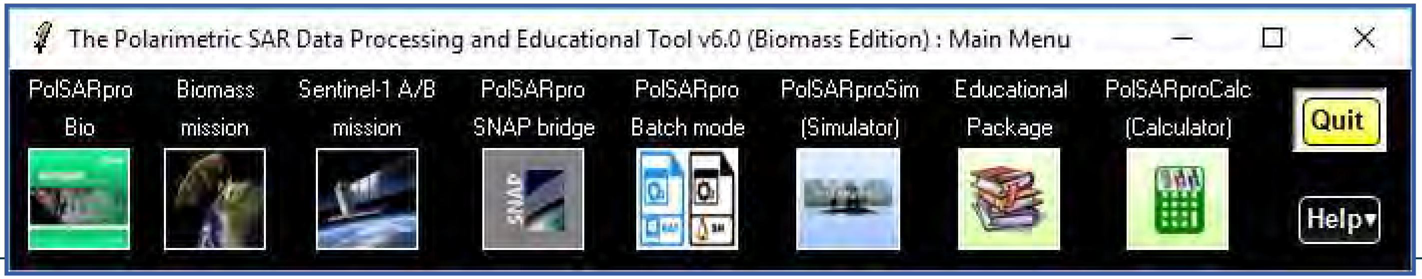

POLSAR-App in PolSARpro – Biomass Edition

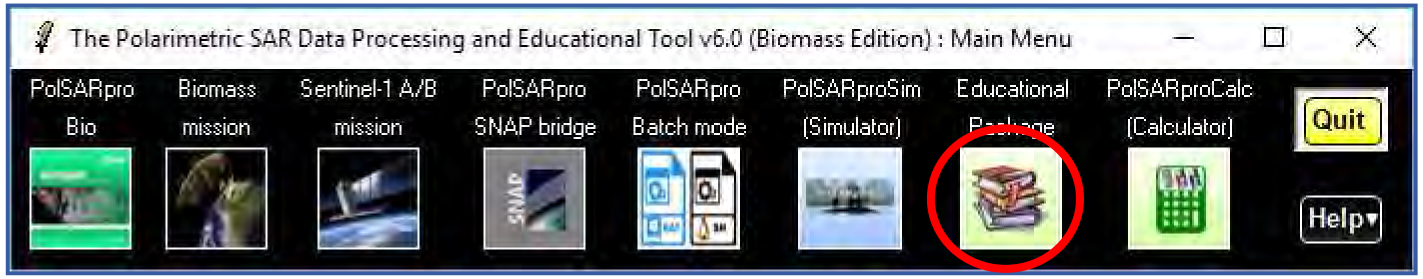

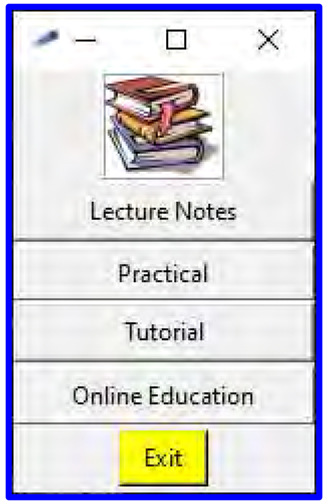

Educational package

POLSAR-App in PolSARpro – Biomass Edition

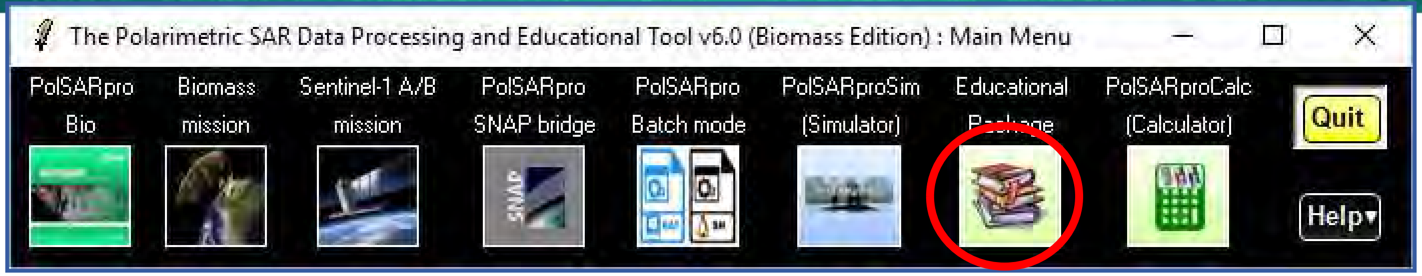

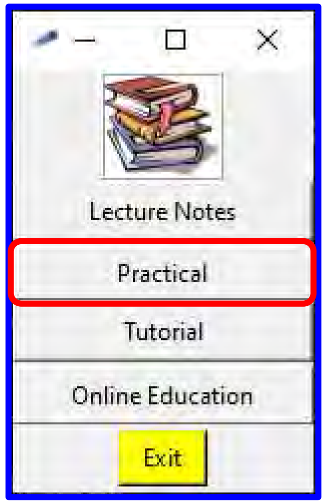

ESA - PolSARap Project

Proposed showcases :

- ✓ ***Agriculture***
- ✓ ***Cryosphere***
- ✓ ***Forest***
- ✓ ***Ocean***
- ✓ ***Urban***

POLSAR-App in PolSARpro – Biomass Edition

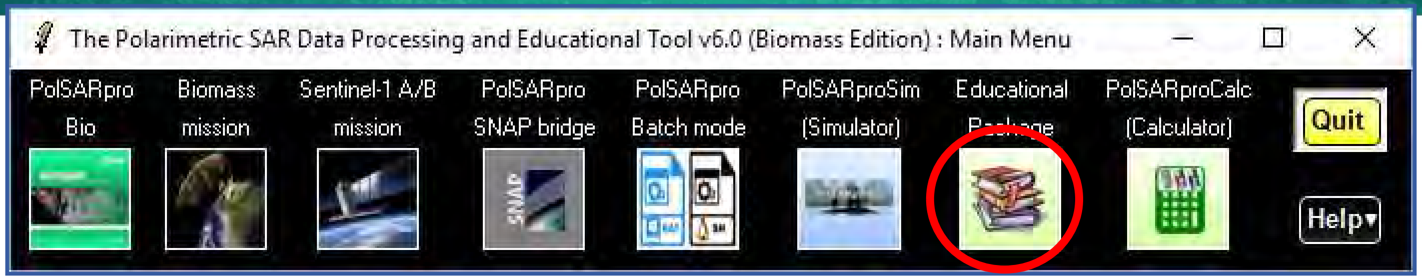

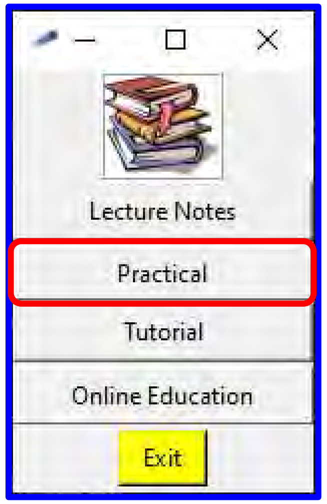


PolSAR-ap Showcase : Agriculture

Input Directory: D:/My_Data_Directory/T3

Output Directory: D:/My_Data_Directory

Init Row: 1 End Row: 1544

Decomposition: ○ Window Size (Row) Window Size (Col)

Surface Soil Moisture Inversion: ● Soil Dielectric Constant Max: 40 Increment Angle of the Incidence Angle LUT (deg)

Dihedral Soil Moisture Inversion: ○ Soil Dielectric Constant Max Increment Angle of the Incidence Angle LUT (deg)

2D-Incidence Angle File: Enter 2D Incidence Angle File

2D Mask File: Enter (showcase_agri_mask.bin) file

Polarimetric Decomposition fs File: Enter (showcase_agri_fs.bin) file

Polarimetric Decomposition Beta File: Enter (showcase_agri_beta.bin) file

Vertical Rougness Indicator (ks) File (optional)

Output Soil Moisture File: D:/My_Data_Directory/showcase_agri_surf_mv_soil.bin

Output Soil Dielectric Constant File: D:/My_Data_Directory/showcase_agri_surf_dc_soil.bin

Output Trunk Dielectric Constant File

PolSAR-ap Showcase : Cryosphere

Input Master - Slave Directory: D:/My_Data_Directory/Master_Dir_Slave_Dir

Output Master - Slave Directory: D:/My_Data_Directory/Master_Dir_Slave_Dir

Init Row: 1 End Row: 900 Init Col: 1 End Col: 1024

Decomposition: ○ Window Size (Row) Window Size (Col)

Inc Ang Unit: ○ Degrees ● Radians

Median Filter: Window Size: 8 Max Nb of Iterations: 3

Inversion: ● Polarization Channel: ● HH ○ HV ○ VV

Ice Dielectric Constant: 2.8 Threshold: 40

Range Pixel Spacing (optional): opt

2D Incidence Angle File: Enter 2D Incidence Angle file

2D Kz File: Enter 2D Kz file

Surface to Volume Ratio File: Enter (showcase_cryo_stv_ratio_HH.bin) file

Complex Coherence File: Enter (cmplx_coh_HH.bin) file

SNR Decorrelation File (optional): Enter SNR Decorrelation file (Optional)

Output Extinction Coefficient File (kappa): D:/My_Data_Directory/Master_Dir_Slave_Dir/showcase_cryo_kappa_HH.bin

Output Penetration Depth File: D:/My_Data_Directory/Master_Dir_Slave_Dir/showcase_cryo_depth_HH.bin

Examples : Agriculture & Cryosphere

Roadmap: methodologies covered here

Change detection

Time series

Target detection

© A. Marino 2021

Notations

- ✓ A **scattering vector** $\underline{k}$ is derived from the complex scattering matrix $[S]$ backscattered by targets in the scene.

- ✓ A **scattering mechanism** or **projection vector** $\underline{\omega}$ is an idealised unitary complex vector pointing at the direction of a potential target in the scene.

- ✓ Given the **covariance** matrix $[C]$ we can use the projection vector $\underline{\omega}$ to evaluate how much **power** a specific scattering mechanism has.
  - ✓ This is done by using **quadratic forms** i.
  - ✓ i is real positive because $[C]$ is Hermitian positive semi-definite

$$\underline{\omega} = \frac{\underline{k}}{\|\underline{k}\|} \qquad [C] = \underline{k} \cdot \underline{k}^{*T} \qquad i = \underline{\omega}^{*T}[C]\underline{\omega}$$

© A. Marino 2021

Ocean: Target detection

Backscattering from the sea: 2 scale model

- ✓ A well established model considers the sea surface as superposition of **short-wave** (capillary) oscillations and **long-wave** (swell) oscillations

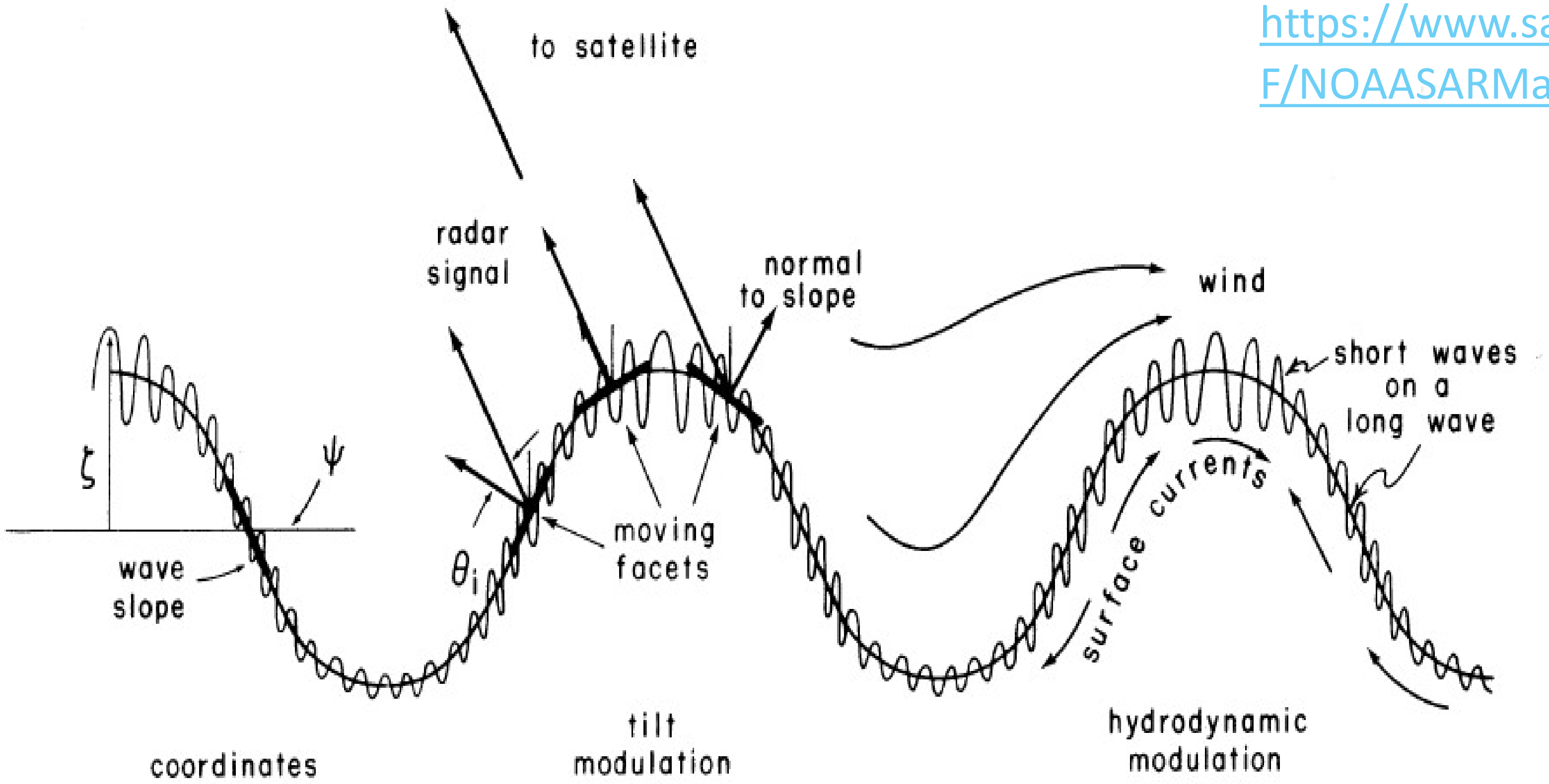

https://www.sarusersmanual.com/ManualPDF/NOAASARManual_CH02_pg025-080.pdf

Backscattering from the sea: Bragg model

- ✓ A regular periodic structure (i.e. wave) allows a **coherent** superposition of reflections from the faces and therefore **constructive** or **destructive** interference

- ✓ 1 water wave produces a strong response at 1 **frequency** and **incidence angle**

- ✓ Since we have a mix of wavelengths/directions there are several frequencies that will be exited**.**

- ✓ If you have no waves, no frequencies are exited

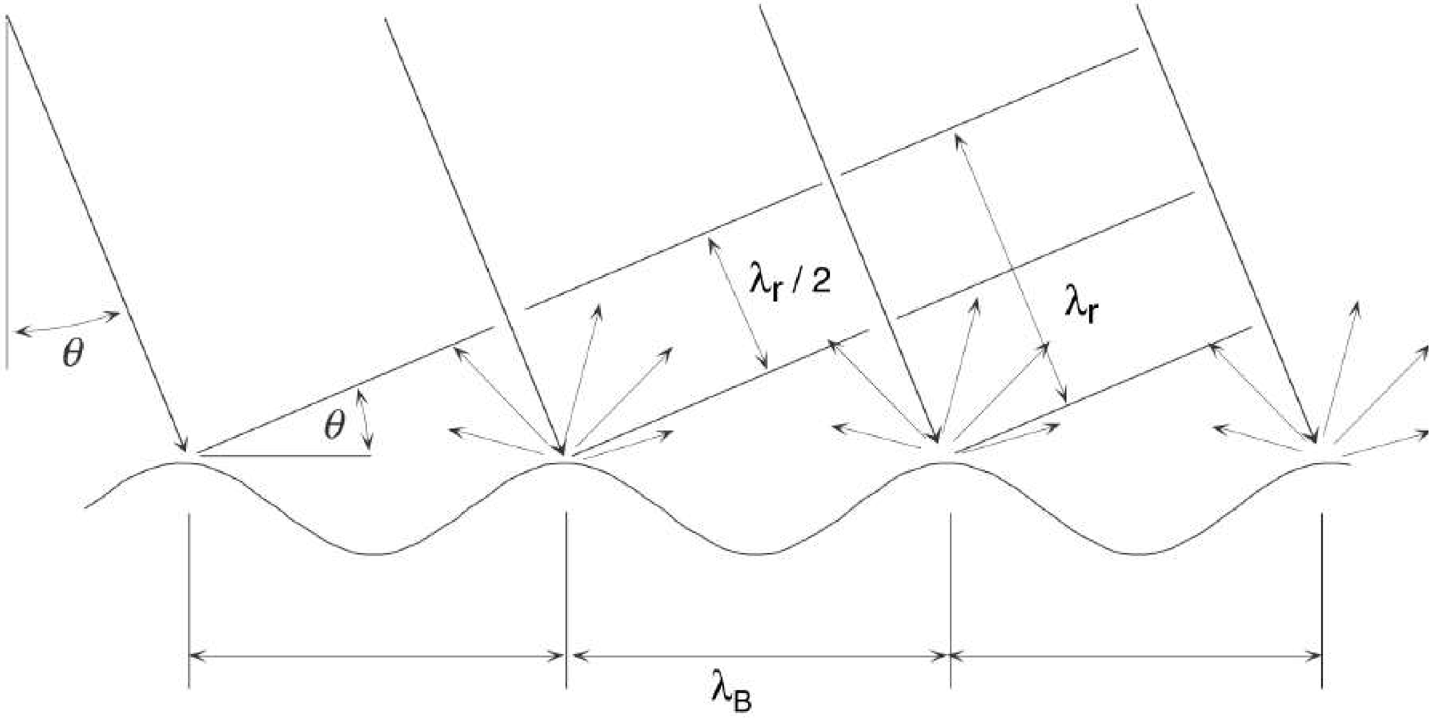

https://www.sarusersmanual.com/ManualPDF/NOAASARManual_CH02_pg025-080.pdf

How PolSAR sees ships

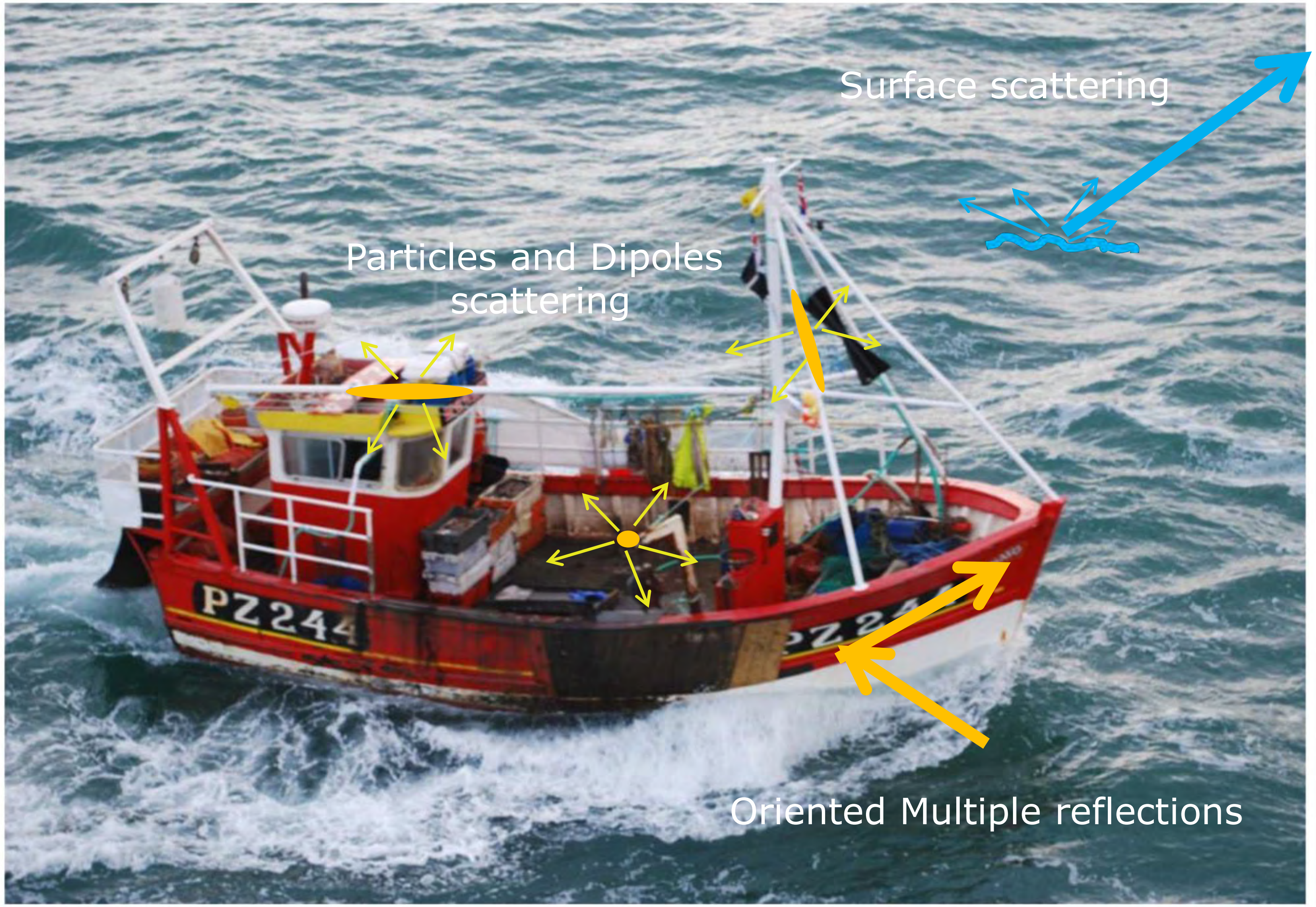

- ✓ The vessel presents a **combination** of scattering mechanisms.
- ✓ The strongest contribution is often expected to be the **double reflection** between the sea surface and the hull or reflections with the surfaces of the bridge

Ships in RADARSAT-2

- ✓ This is a RADARSAT-2 quad-pol acquisition near Portsmouth, UK, 2011
- ✓ Are ships single or partial targets?

Canadian Space Agency and MDA® 2011

Ships in RADARSAT-2

- ✓ This is a RADARSAT-2 quad-pol acquisition near Portsmouth, UK, 2011
- ✓ Are ships single or partial targets?
- ✓ In phenomenologically, it depends on the size of the vessel and how many pixels contains.
- ✓ Physically, they are generally a collection of single targets.

Canadian Space Agency
and MDA® 2011

Target detection theory

Target detection

The idea is to identify
“something different”
inside an image
(as in the game **Spot the Sith**).

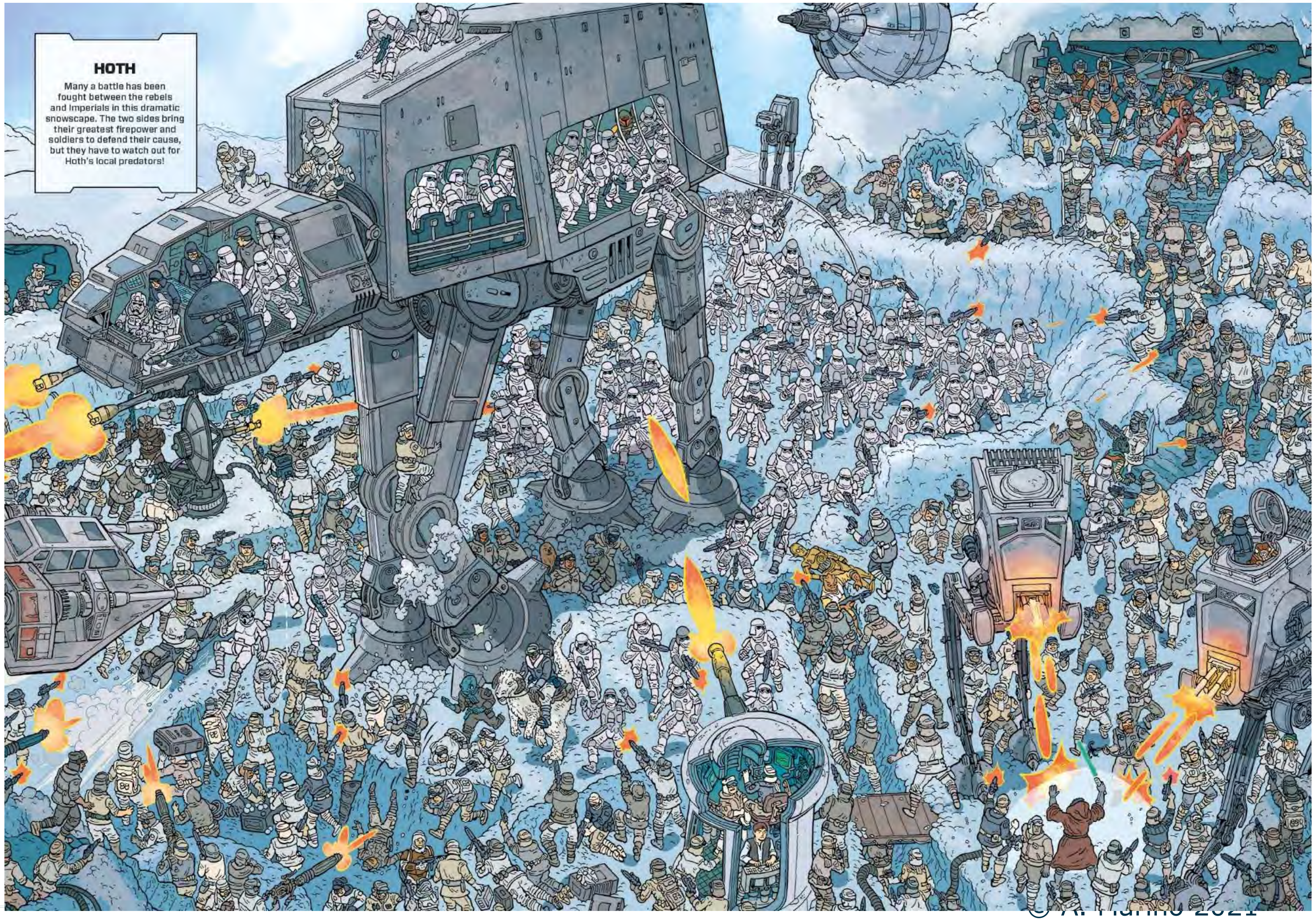

HOTH

Many a battle has been fought between the rebels and Imperials in this dramatic snowscape. The two sides bring their greatest firepower and soldiers to defend their cause, but they have to watch out for Hoth's local predators!

Detection Theory

- ✓ If we want to make a detector we need to set a **threshold**.

- ✓ Once we set a threshold, we can define the **probability**
  - ✓ that we can detect the ship: **Probability of Detection** $P_{d;}$
  - ✓ that we detect a region without a ship: **Probability of False Alarm** P_f.

- ✓ We these probability we can build a **Error Matrix**

Hit	Miss
False alarm	Correct reject

Kay, S. M.
Fundamentals of Statistical Signal Processing
Prentice Hall, Upper Saddle River, US, **1993**

Single pol detectors

$$I = \left\langle | img |^2 \right\rangle < T \qquad I \sim Exp(\lambda)$$

Cell Averaging – Constant False Alarm Rate (CA-CFAR):

$$T = \langle |img|^2 \rangle_{train} \cdot f$$

It can be derived analytically

- ✓ These detectors generally set an adaptive threshold on the intensity image
- ✓ CA-CFAR uses a training area to identify the distribution of the clutter and set a threshold base don the probability of false alarms

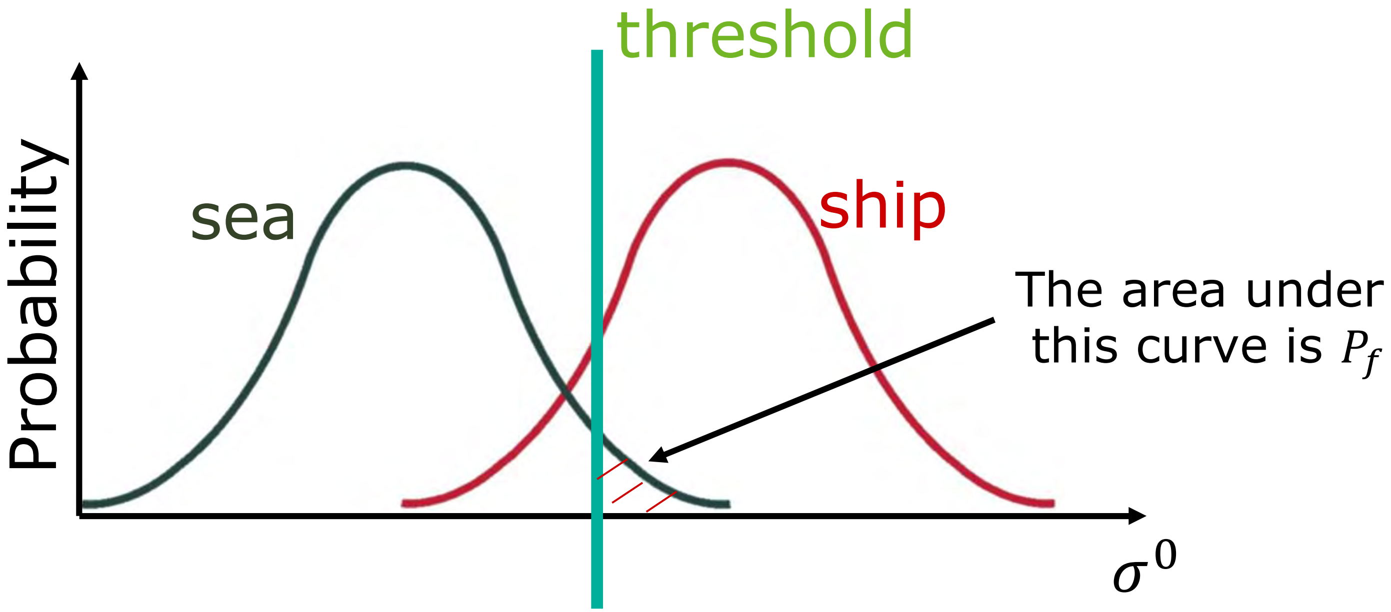

The area under this curve is P_f

Guard windows

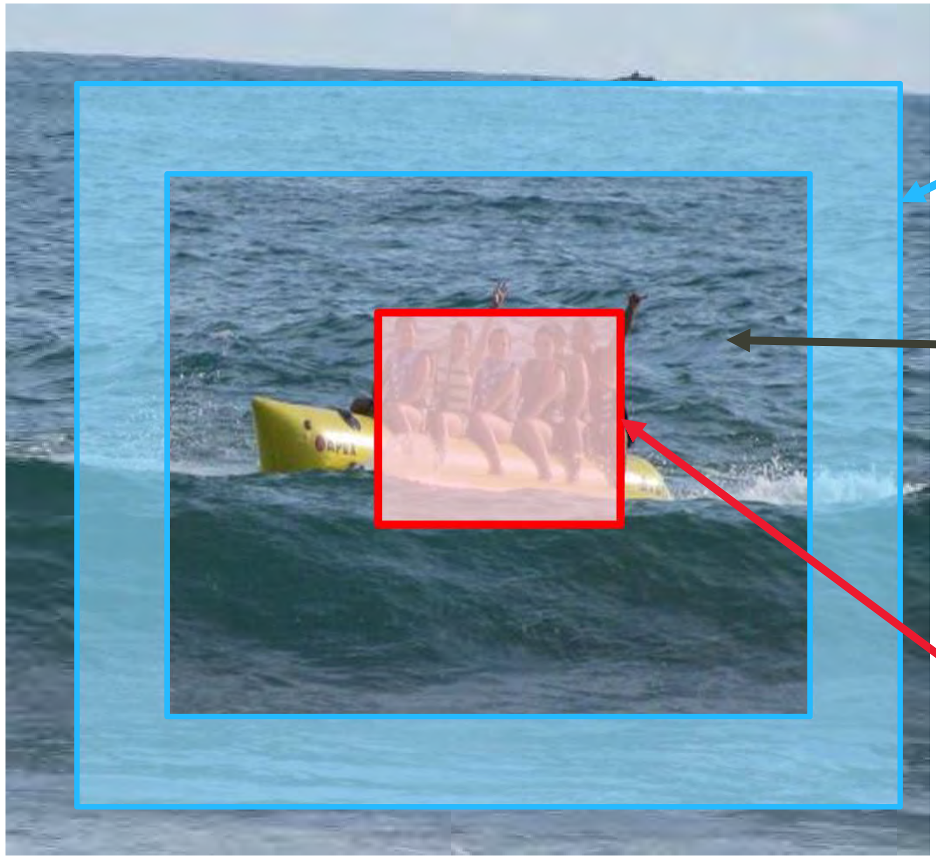

$\langle|img|^2\rangle_{train}$

Training window:
pixels used for training

Guard window:
pixels not used

$\langle|img|^2\rangle_{test}$

Test window:
pixels used for testing

Pol-SAR target detectors

A) Cloude-Pottier Entropy

- ✓ It has been shown that the **sea** has a low entropy because is it rather polarised (it is all a surface)
  - ✓ Notice, the sea is distributed but single, which is not a very common property

- ✓ **Ships** are a collection of single targets and therefore their entropy is high
  - ✓ On a averaging window they show a "confused" polarimetric behaviour (although each of the pixels may be "single")

$$I = \underline{\omega}^{*T}[T]\underline{\omega} \geq 0$$

$$[T]=[U][\Sigma][U]^{*T} = \sum_{i=1}^{3} \lambda_i \underline{u}_i \underline{u}_i^{*T} = \lambda_1 \underline{u}_1 \underline{u}_1^{*T} + \lambda_2 \underline{u}_2 \underline{u}_2^{*T} + \lambda_3 \underline{u}_3 \underline{u}_3^{*T}$$

$$[T]=\begin{bmatrix} \langle |k_1|^2 \rangle & \langle k_1 k_2^* \rangle & \langle k_1 k_3^* \rangle \\ \langle k_2 k_1^* \rangle & \langle |k_2|^2 \rangle & \langle k_2 k_3^* \rangle \\ \langle k_3 k_1^* \rangle & \langle k_3 k_2^* \rangle & \langle |k_3|^2 \rangle \end{bmatrix}$$

$$[U]^{*T}[U]=[I] \Rightarrow [U]^{*T}=[U]^{-1}$$

Unitary matrix

Eigenvalues

Eigenvectors

A) Cloude-Pottier Entropy

We can define a **probability** of each eigenvalue:

$$P_i = \frac{\lambda_i}{\lambda_1 + \lambda_2 + \lambda_3}$$

We can calculate the **Entropy**:
of the scattering process

$$\boxed{H = \sum_{i=1}^{3} \left(-P_i \log_3 P_i \right)}$$

Cloude, S. R. & Pottier, E.
An Entropy Based Classification Scheme for Land Applications of Polarimetric SAR
IEEE Transactions on Geoscience and Remote Sensing, **1997**, *35*, 68-78

B) Polarimetric Notch Filter

- ✓ In this detector we isolate the power contribution coming from the sea along one dimension and look at the **perpendicular subspace**, which we define as the target subspace.

- ✓ In order to work with partial targets we first build a partial feature target starting from the covariance matrix

$$\underline{t}=\mathrm{Trace}([\mathrm{C}]\Psi) = [\langle|k_1|^2\rangle, \langle|k_2|^2\rangle, \langle|k_3|^2\rangle, \langle k_1^* k_2\rangle, \langle k_1^* k_3\rangle, \langle k_2^* k_3\rangle]^T$$

You can also express this using quadratic forms

$$\underline{t}=\left[\underline{\omega}_1^{*T}[C]\underline{\omega}_1, \underline{\omega}_2^{*T}[C]\underline{\omega}_2, \underline{\omega}_3^{*T}[C]\underline{\omega}_3, \underline{\omega}_1^{*T}[C]\underline{\omega}_2, \underline{\omega}_1^{*T}[C]\underline{\omega}_3, \underline{\omega}_2^{*T}[C]\underline{\omega}_3\right]^T$$

B) Polarimetric Notch Filter

$$\underline{t}_{sea} = \left[[T_{sea}]_{11}, [T_{sea}]_{22}, [T_{sea}]_{33}, [T_{sea}]_{12}, [T_{sea}]_{13}, [T_{sea}]_{23}\right]^T$$

$$P_{Sea} = \left\langle \left| \underline{t}^{*T} \cdot \hat{\underline{t}}_{Sea} \right|^2 \right\rangle \qquad P_T = P_{tot} - P_{Sea} \qquad P_{tot} = \left\langle \underline{t}^{*T} \cdot \underline{t} \right\rangle$$

- ✓ These vectors are included in the **perturbation filter coherence**, omitting the power from the target.
  - ✓ More info on this later

$$\boxed{\gamma_n = \frac{1}{\sqrt{1 + RedR \dfrac{1}{\left\langle \underline{t}^{*T} \cdot \underline{t} \right\rangle - \left\langle \left| \underline{t}^{*T} \cdot \hat{\underline{t}}_{sea} \right|^2 \right\rangle}}}}$$

Marino, A. A Notch Filter for Ship Detection With Polarimetric SAR Data *IEEE Journal of Selected Topics in Applied Earth Observations and Remote Sensing*, **2013**, *6*, 1219 - 1232

C) Polarimetric Match Filter

- ✓ We try to optimise the contrast between the sea clutter and the target to detect
- ✓ Novak PMF is based on the Generalised Rayleigh Quotient proposed by Fisher:

$$\boxed{\rho_c = \frac{\underline{\omega}^{*T}[T_{tar}]\underline{\omega}}{\underline{\omega}^{*T}[T_{sea}]\underline{\omega}} = \frac{P_{target}}{P_{sea}}}$$

We can optimize it using a **Lagrange** constrained optimization:

$$L = \underline{\omega}^{*T}[T_{tar}]\underline{\omega} - \lambda\left(\underline{\omega}^{*T}[T_{sea}]\underline{\omega} - Const\right)$$

$$\frac{\partial L}{\partial \underline{\omega}^{*T}} = [T_{tar}]\underline{\omega} - \lambda[T_{sea}]\underline{\omega}$$

$$\boxed{[T_{sea}]^{-1}[T_{tar}]\underline{\omega} = \lambda\underline{\omega}}$$

Novak, L.; Burl, M. & Irving, W.W., Optimal Polarimetric Processing for Enhanced Target Detection, *IEEE Transactions on Aerospace and Electronic Systems*, **1993**, *29*, 234-244

D) Multilook Polarimetric Whitening Filter

- ✓ We want to **whiten** the stochastic process, i.e. we remove the structure of the covariance matrix, so that the vector generated by that process will be Gaussian White (i.e. each of the complex components of the processed scattering vector has the same unitary variance).

- ✓ This comes from the idea of Novak, who was trying to obtain an image with the **lowest possible speckle**

$$\underline{w} = T_c^{-1/2}\underline{k} \qquad int_1 = \left(T_c^{-\frac{1}{2}}\underline{k}\right)^{*T} \cdot \left(T_c^{-\frac{1}{2}}\underline{k}\right) = \underline{k}^{*T}T_c^{-1}\underline{k}$$

$$int_1 = Trace\left\{\underline{k}^{*T}T_c^{-1}\underline{k}\right\} = Trace\left\{T_c^{-1}\underline{k}\,\underline{k}^{*T}\right\} = Trace\{T_c^{-1}T\}$$

Novak, L.; Burl, M. & Irving, W.W., Optimal Polarimetric Processing for Enhanced Target Detection, *IEEE Transactions on Aerospace and Electronic Systems*, **1993**, *29*, 234-244

D) Multilook Polarimetric Whitening Filter

- ✓ Then it was proposed to “whiten” the test pixels by the covariance matrix of the training pixels.
- ✓ If we have homogeneous clutter, the output will be a unitary vector, otherwise if the structure of the target covariance matrix $[T]$ is rather orthogonal to the clutter $[T_c]$ we have that the orthogonal components will be amplified by producing a vector with a much larger magnitude
- ✓ Including some average makes the output more robust

$$int_N = \sum_{i=0}^{N} Trace\{T_c^{-1}T\}$$

Guoqing Liu; Shunji Huang; A. Torre; F. Rubertone, The multilook polarimetric whitening filter (MPWF) for intensity speckle reduction in polarimetric SAR images, IEEE Transactions on Geoscience and Remote Sensing, 36(3) 1998.

E) Reflection Symmetry

- The **reflection symmetry** in a **pixel** dictates that the left and right parts of the target are the same. This generally translates into a lack of overall orientations in a target.
- For a **stochastic process**, we want that in average this property is valid over the whole pixels in the averaging cell.
- **Phenomenologically**, reflection symmetry leads to a null correlation between the co- and cross-polarisation channels.
- The sea is an horizontal surface and it is reflection symmetric, while ships and other complex targets at see are not expected to have reflection symmetry

$$RF_1 = |\langle S_{HH} S_{HV}^{*} \rangle|$$

$$RF_2 = |\langle S_{VV} S_{VH}^{*} \rangle|$$

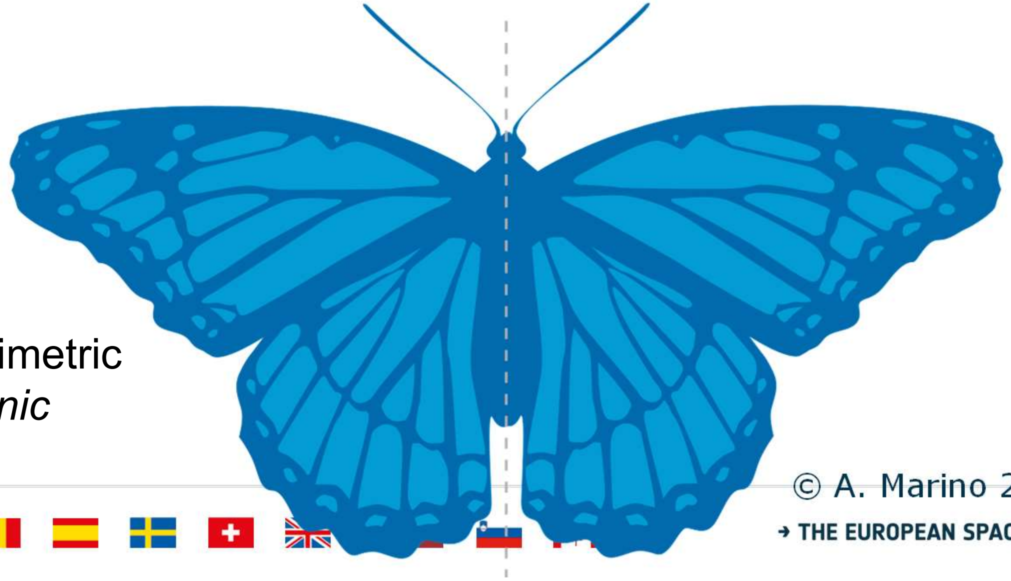

Nunziata, F.; Migliaccio, M. & Brown, C., Reflection symmetry for polarimetric observation of man-made metallic targets at sea, *IEEE Journal of Oceanic Engineering*, **2012**, *37*, 384-394

Results on data: PolSAR-App

- ✓ In PolSAR-App several polarimetric detectors were tested over ALOS quad-pol acquisitions near Tokyo.
- ✓ Validation data where present with AIS and ground radars

Tokio Bay, Japan

ALOS-PalSAR

©JAXA 2009

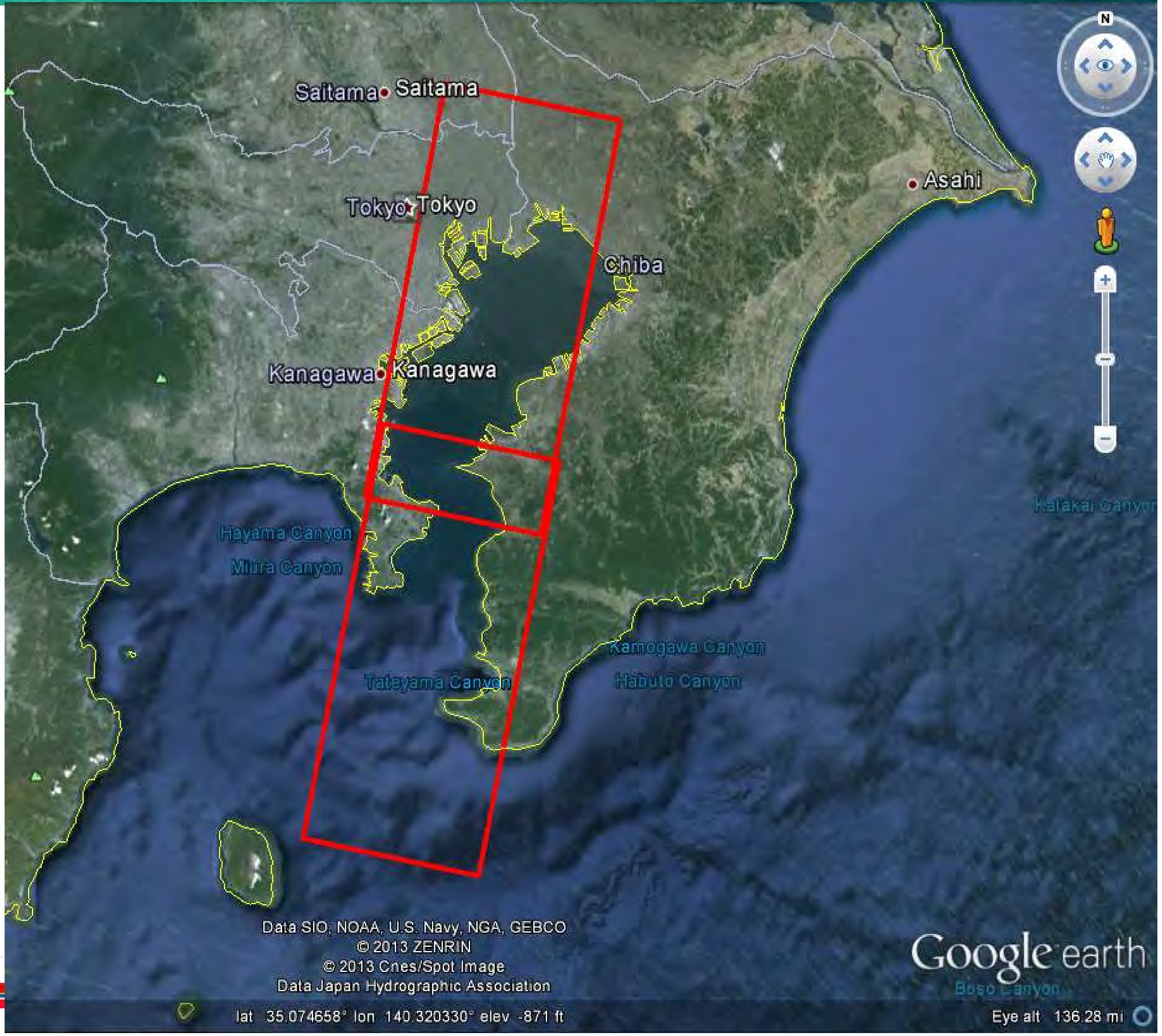

Ship detection: ALOS-2 quad-pol data

Pauli RGB

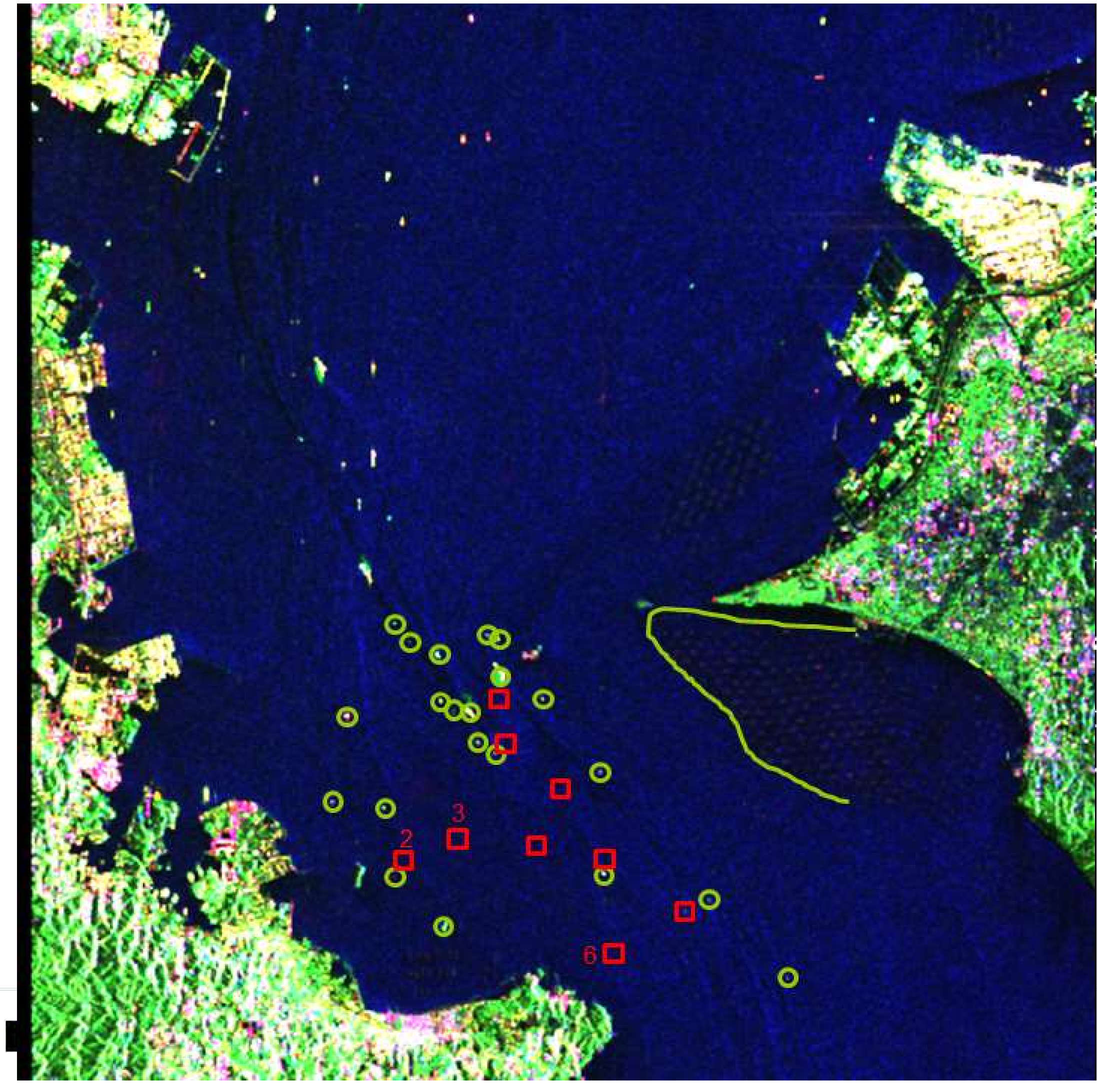

HV intensity

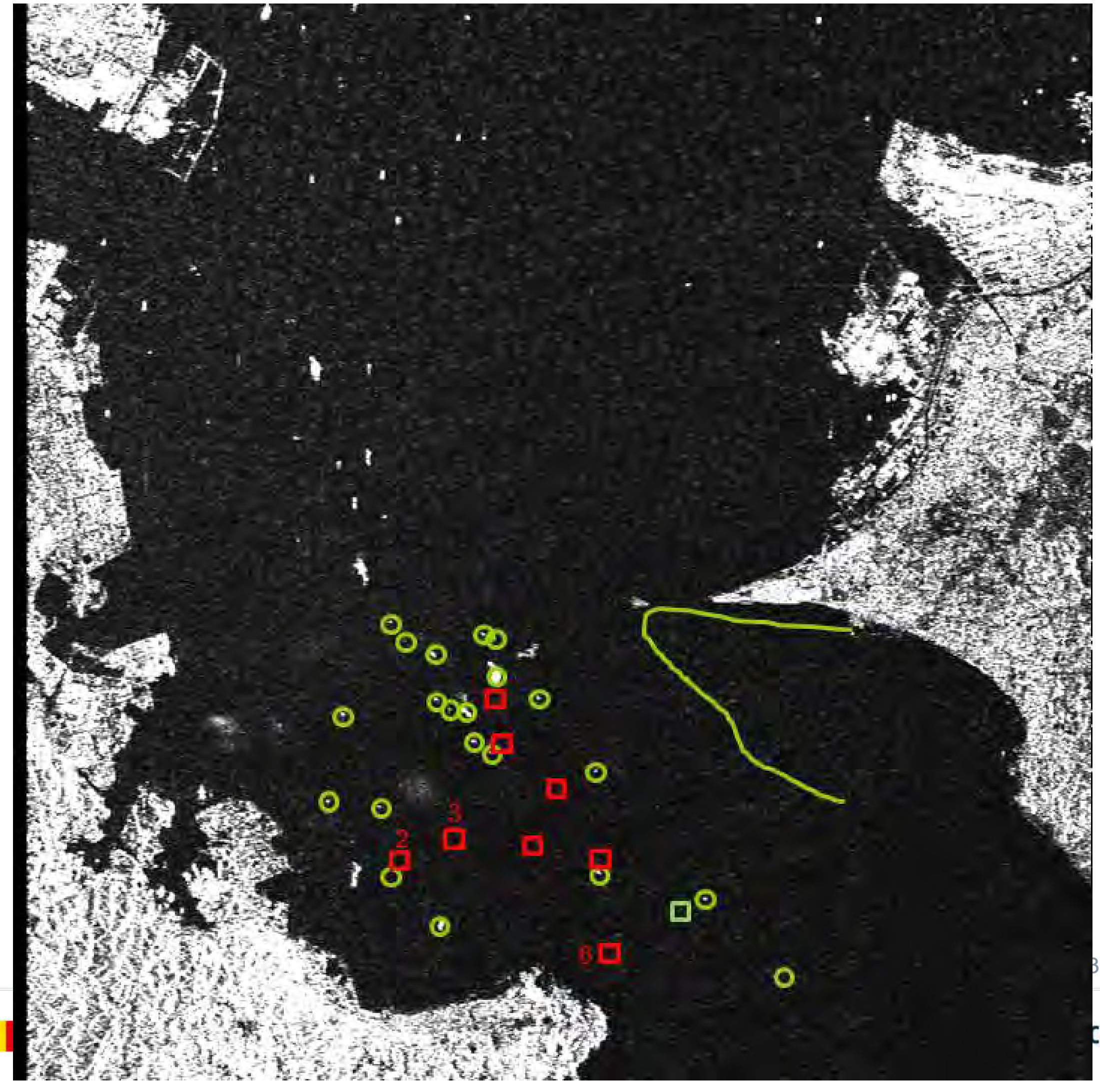

Ship detection: ALOS-2 quad-pol data

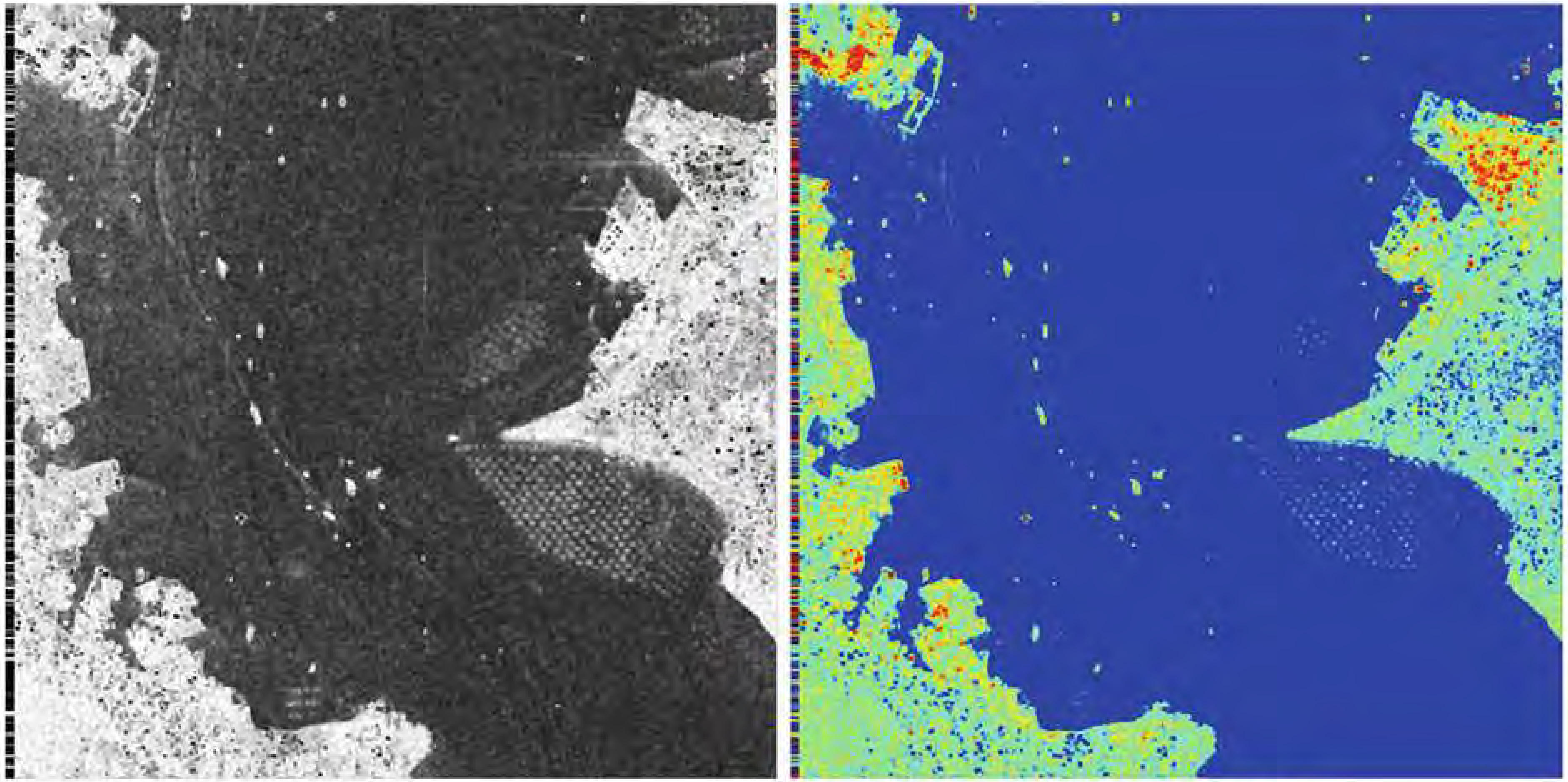

(a) Entropy (b) Averaged α

© A. Marino 2021

Ship detection

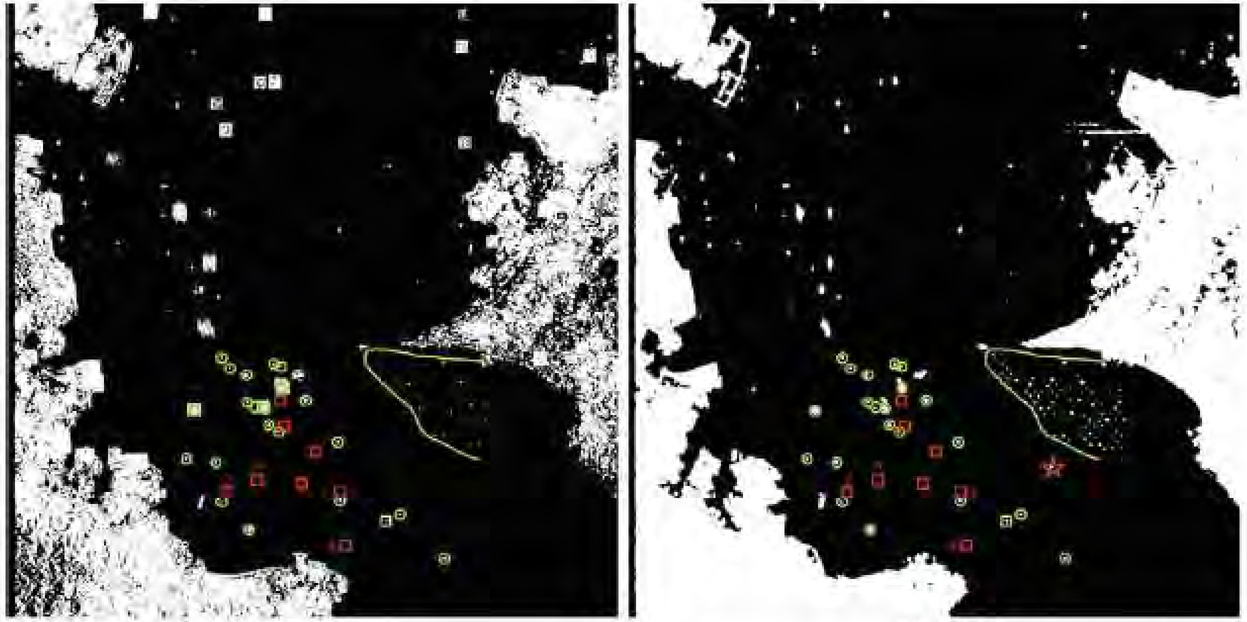

(a) GP-PNF

(b) PMF

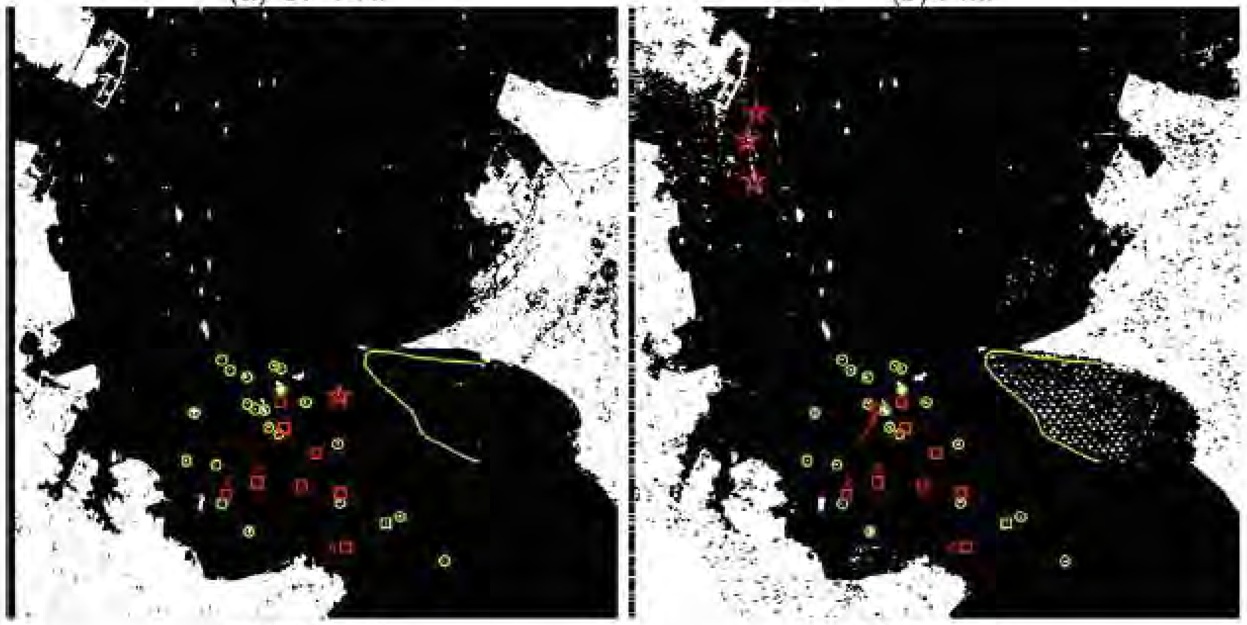

(c) Liu et al.

(d) Entropy

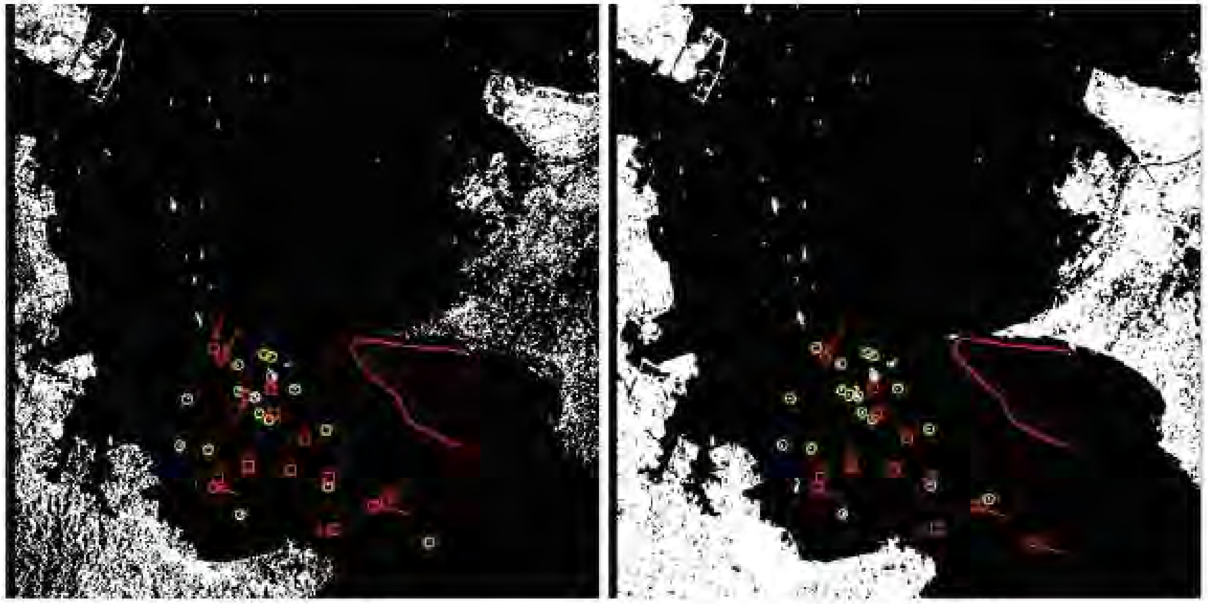

(a) Symmetry

(b) HV intensity

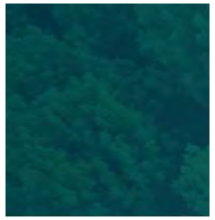

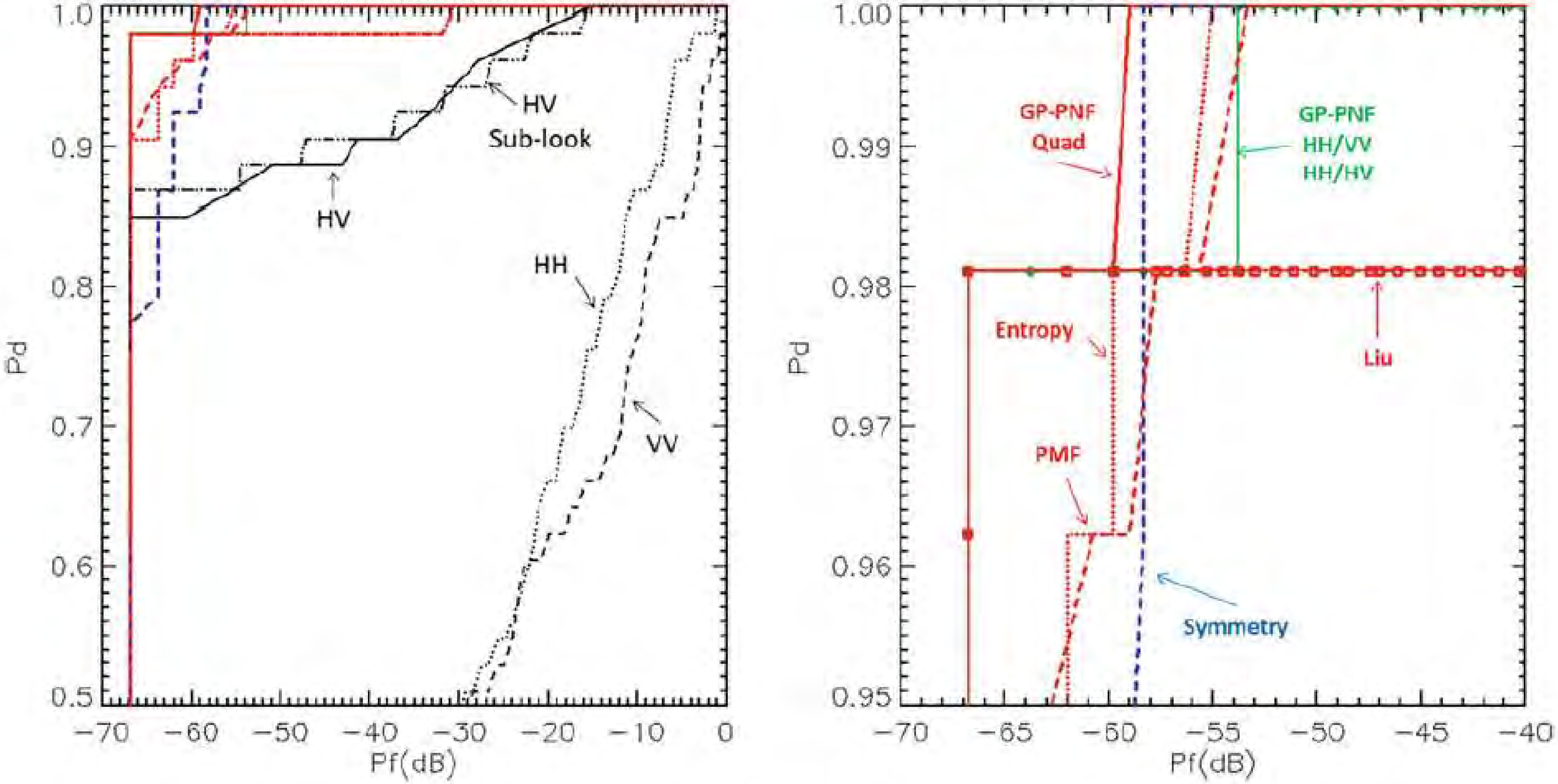

Fig. 6.14 ROC curves for the different detectors: red solid, GP-PNF quad-pol; red dotted, Cloude-Pottier entropy; red dashed, PMF; red squares, Liu et al.; blue dashed, symmetry VV/VH; green solid, dual-pol HH/VV GP-PNF; green diamonds, dual-pol HH/HV GP-PNF; black solid, HV intensity; black dotted, HH intensity; black dashed, VV intensity; black dot dash, cross-correlation of sub-look images in HV. (**b**) Presents a zoom of (**a**) in the upper left area. Best detection is in the upper left area of the plot

Forestry, urban: Change detection

Change detection with PolSAR

- ✓ If we perform repeated visits on areas, we can also observe changes to that area.
- ✓ Now we have more polarimetric acquisitions:

First polarimetric acquisition

$\underline{k}_1$

$\underline{k}_2$

Second polarimetric acquisition

Change detection with PolSAR

✓ Change detectors using the interferometric phase are often referred to as **Coherent** detectors

✓ Change detectors based only on the covariance matrix [C] are called **Incoherent** detectors

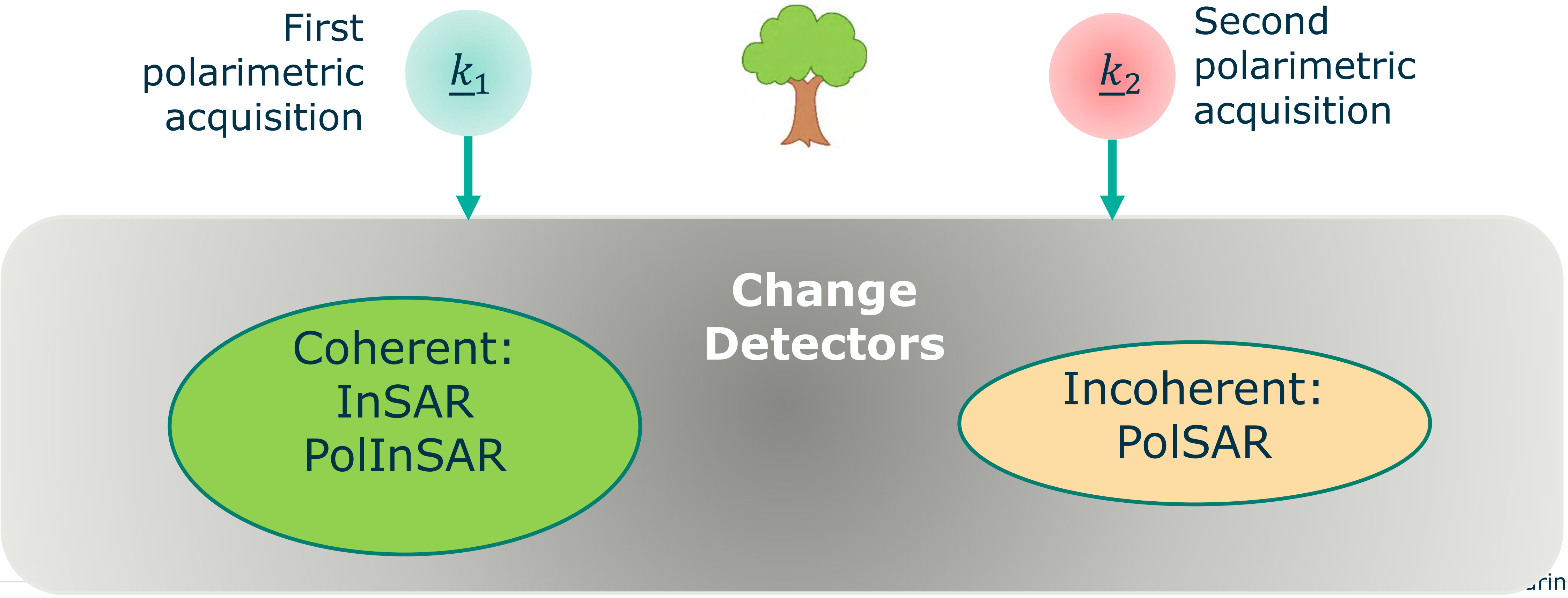

First polarimetric acquisition

$\underline{k}_1$

Second polarimetric acquisition

$\underline{k}_2$

Change Detectors

Coherent:
InSAR
PolInSAR

Incoherent:
PolSAR

Spot the difference

- ✓ These detectors often boil down to identify what changed from one image to the other (as in the game **Spot the Difference**).

Random Variables: reminder (1)

A Random Variable (r.v.) is a variable whose value is subject to statistical variation.

Refreshing your memory:
Example: a r.v. is the result of throwing a **dace**. For each throw it can assume 6 different possible values (1 to 6). Each time we throw there is no way to know what is coming out (unless your dace is loaded!!!).

Definitions:

- **Realisation (or observed value)**: each single result of throwing the dace
- **Probability Density Function, pdf:** a function that describes the statistical behaviour of a r.v.
- **Mean value (or expected value)**: the central tendency of a r.v.
- **Variance**: a measure of how the observed values are spread out around the expected value

Random Variables: reminder (2)

Ideal Mathematical World

x: Random Variable

$f_X(x)$: pdf ➡ $\int_{-\infty}^{\infty} f_X(x)dx = 1$

Pdf has unitary area (the are distribution of probability therefore the sum to 1)

Expected value

$$E[x] = \int_{-\infty}^{\infty} x f_X(x)dx$$

Variance

$$VAR[x] = \int_{-\infty}^{\infty} (x - E[x])^2 f_X(x)dx$$

Real World: In the real world, we do not have infinite realisations of our r.v. and we need to perform some estimation over a limited (finite) number of samples.

Mean value estimator

$$\mu = \frac{1}{N}\sum_{i=1}^{N} x_i$$

Variance estimator

$$\sigma^2 = \frac{1}{N}\sum_{i=1}^{N} (x - \mu)^2$$

Random Variables and SAR

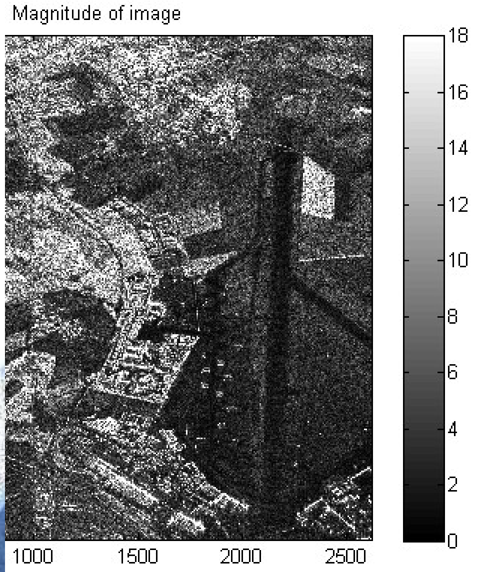

Random Variables and SAR

- ✓ The **interaction** between the incident wave and the targets has a strong component of randomness.

- ✓ In the same resolution cell there is a LARGE number of scatterers (as a “role of thumb”, the wave interacts strongly with objects with dimensions bigger or comparable with the wavelength).

- ✓ The resolution cells are of the order of meter(s). The wavelength is of the order of (tens of) centimeters --> **many scatterers** in the same resolution cell!!

- ✓ So… what is the problem having a lot of scatteres interacting together?
- ✓ For the linearity of Maxwell equations, the wave is the **superimposition** of the waves coming from each single scatterer.

- ✓ **Can you see where the problem is?**

Why statistical variation (explained)?

Imagine this is a single resolution cell
with (x,y) coordinates in the image

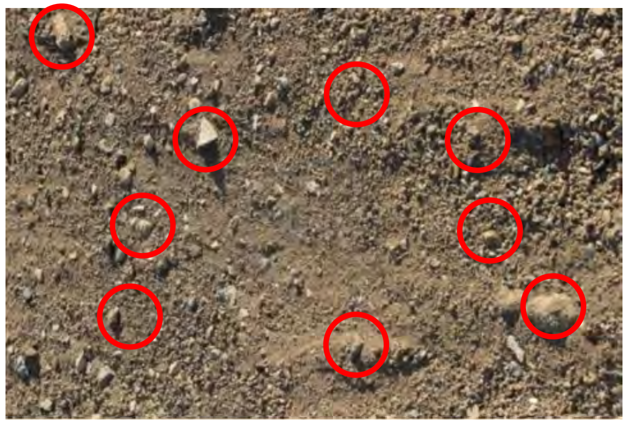

$\uparrow\ E_i \in C$

$$\uparrow\ E(x,y) = \sum_{i=1}^{N(x,y)} E_i$$

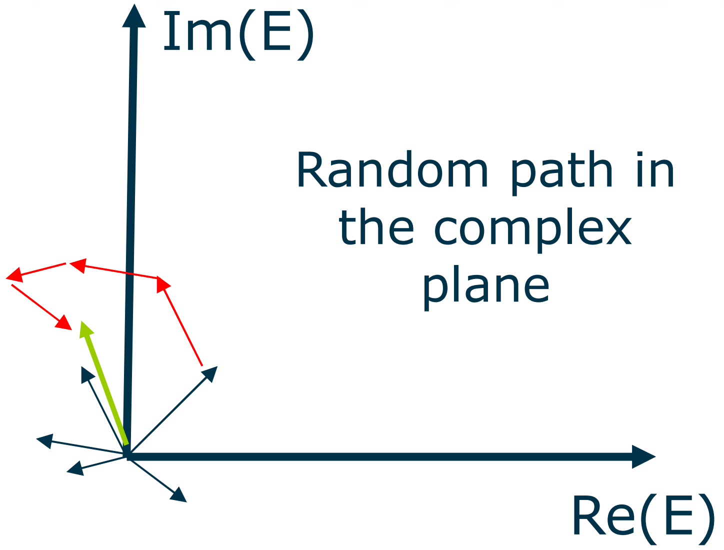

Random path in the complex plane

Def. **Speckle** = The **coherent sum** (*interference*) of scatterer returns in the *same resolution cell*

It makes image ***interpretation*** and ***retrieval*** of parameters very complex

One observable (superimposition of many scatterers) $\longrightarrow$ $E(x,y) = \sum_{i=1}^{N(x,y)} E_i$ $\longleftarrow$ N unknown

Putting it into math: pdf

The single pixel is one random realisation of a random variable.

$$E(x,y)=\sum_{i=1}^{N(x,y)} E_i$$

Mean

Standard Deviation

The *pdf* of the complex SAR pixel is modelled as a **Circular Symmetric Complex Gaussian**

$$Re\{E\}, Im\{E\} \sim N(0,\sigma)$$

Mean

The *pdf* of the magnitude is **Rayleigh**

$$|E| \sim Rayleigh(\tau)$$

The *pdf* of the phase is **Uniform**

$$\arg\{R\} \sim \Pi\ (-\pi,\pi)$$

The *pdf* of the intensity (or power, or energy) is **Exponential**

$$|E|^2 \sim Exp(\tau^2)$$

Details on pdf‘s

Gaussian distribution:

$Re\{E\}, Im\{E\} \sim N(0, \sigma)$

$$f_{\mathrm{Re}}(re) = \frac{1}{\sqrt{2\pi\sigma}} e^{-\frac{re^2}{2\sigma^2}}; \; f_{\mathrm{Im}}(im) = \frac{1}{\sqrt{2\pi\sigma}} e^{-\frac{im^2}{2\sigma^2}}$$

$$E[re] = E[im] = 0 \qquad VAR[re] = VAR[im] = \sigma^2$$

Rayleigh distribution:

$|E| \sim Rayleigh(\tau)$

$$f_M(m) = \frac{m}{\sigma^2} e^{-\frac{m^2}{2\sigma^2}} u(m)$$

$$E[m] = \sigma\sqrt{\frac{\pi}{2}} \qquad VAR[m] = \frac{4-\pi}{2}\sigma^2$$

Details on pdf‘s

Uniform distribution:

$$\arg\{R\} \sim \Pi\,(-\pi, \pi)$$

$$f_\Phi(\varphi) = \begin{cases} \dfrac{1}{2\pi} & \text{for } \varphi \in [-\pi, \pi] \\ 0 & \end{cases}$$

$$E[\varphi] = (\pi - \pi)/2 = 0 \qquad VAR[\varphi] = \frac{(\pi + \pi)^2}{12} = \frac{\pi^2}{3}$$

Exponential distribution:

$$f_W(w) = \frac{1}{2\sigma^2} e^{-\frac{w}{2\sigma^2}} u(w)$$

$$|E|^2 \sim Exp(\lambda) = Exp\left(\frac{1}{2\sigma^2}\right)$$

$$E[w] = \lambda^{-1} = 2\sigma^2 \qquad VAR[w] = \lambda^{-2} = 4\sigma^4$$

Pdf derivation

✓ FROM **Complex Gaussian** distribution TO **Rayleigh and Uniform distributions**

✓ It is possible to derive the Rayleigh, Uniform and Exponential distribution starting from complex Gaussian pixels:

1. Change of coordinates Cartesian to Polar
2. Theorem of transformation of random variable 2->2 (Cartesian to Polar coordinates).
3. Integration to go from joint to single pdf (to remove one of the variables from the joint pdf)

Talking about noise

- ✓ Since the speckle makes the image interpretation harder, some people talk of it as **Noise**.

- ✓ In particular, it can be demonstrated that given the intensity of a SAR image, we can write it as:

$$I = I_0 \sigma_{exp} \qquad \sigma_{exp} \sim Exp(1)$$

where I_0 is the expected value (actual value) of the intensity. σ is an exponential random variable with unitary mean. Since we multiply the actual value by a random variable, the noise is defined “**multiplicative**”.

- ✓ In actual fact, the speckle is linked to the very same nature of radar backscattering and therefore it should not be defined as noise… i.e. the noise itself is our signal :)

What about the classic additive noise????

- ✓ Of course we also have some **additive noise** due to circuitry and antennas
- ✓ The *pdf* of the additive white (thermal) noise is **Circular Symmetric Complex Normal**

$$n \sim N(0, \sigma_n)$$

$$E(x,y) = \sum_{i=1}^{N(x,y)} E_i + n$$

- ✓ A Signal to Noise Ratio can be calculated as: $SNR = \frac{|E|^2}{|n|^2}$
- ✓ As long as the **SNR** is high, we can neglect the effect of the thermal noise on the characterisation of the SAR images. But when the backscattering is very low and close to the **noise floor** (noise level of the instrument) then the additive noise should be taken into account in our polarimetric analysis

Examples of noise on photo

Original

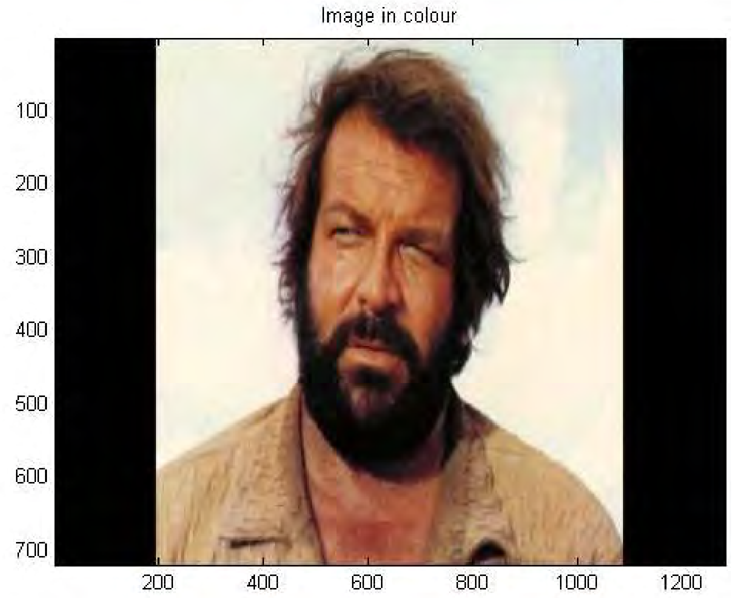
Image in colour

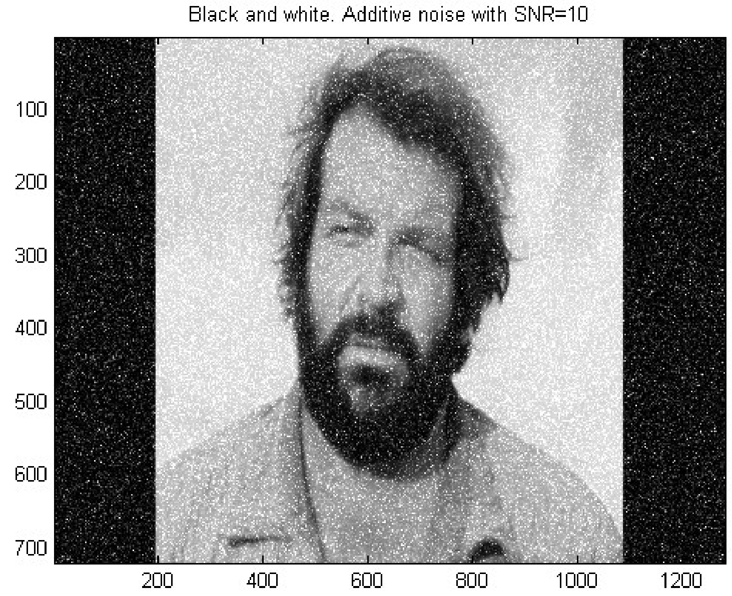
Black and white. Additive noise with SNR=10

Additive
SNR=10

Additive
SNR=2

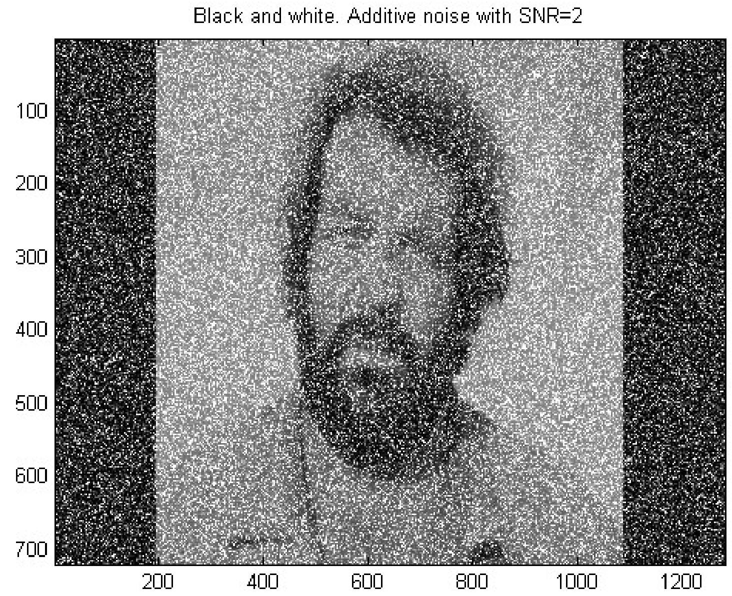
Black and white. Additive noise with SNR=2

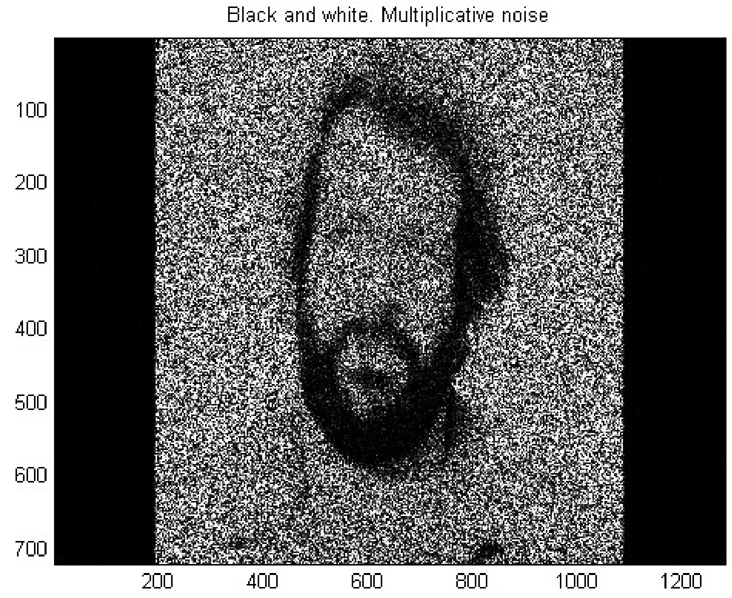
Black and white. Multiplicative noise

Multiplicative

Why averaging helps?

Advantages:

✓ It helps to **reduce the statistical variation** around a defined mean value.

✓ If performed properly it will not affect the mean value (which is what we want to retrieve)

Disadvantages:

✓ if the pixels you average belongs to different targets (e.g. forest and a road in the forest) than the results is not very meaningful

✓ It may reduce the resolution because many pixels are used to obtain a single value, although if done with adaptive algorithm it may still preserve the resolution for point targets and edges

Can we average the complex pixels (Gaussian pdf)? NOOOOO!

We want to ***reduce* the speckle**… i.e. the statistical variation

The return from the j pixel is a **Circular Symmetric Complex Normal** $E \sim N_c(0, \sigma)$

Will we reduce the variance by averaging several complex pixels?

NOOOOO!

The resulting random variable is still a **complex Normal**

$$E_1 \sim N_c(0, \sigma_1)$$
$$E_2 \sim N_c(0, \sigma_2)$$

$$\frac{E_1 + E_2}{2} \sim N_c\left(0, \frac{\sigma_1 + \sigma_2}{4}\right) \quad \xrightarrow[\sigma_1 = \sigma_2 = \sigma]{\text{If homogeneous}} \quad \frac{E_1 + E_2}{2} \sim N_c\left(0, \frac{\sigma}{2}\right)$$

We average intensity: Gamma distribution

Pdf: $$f_I\left(I \mid L, E[I]\right) = \frac{L^L}{E[I]\Gamma(L)}\left[\frac{I}{E[I]}\right]^{L-1}\exp\left[-\frac{LI}{E[I]}\right]$$

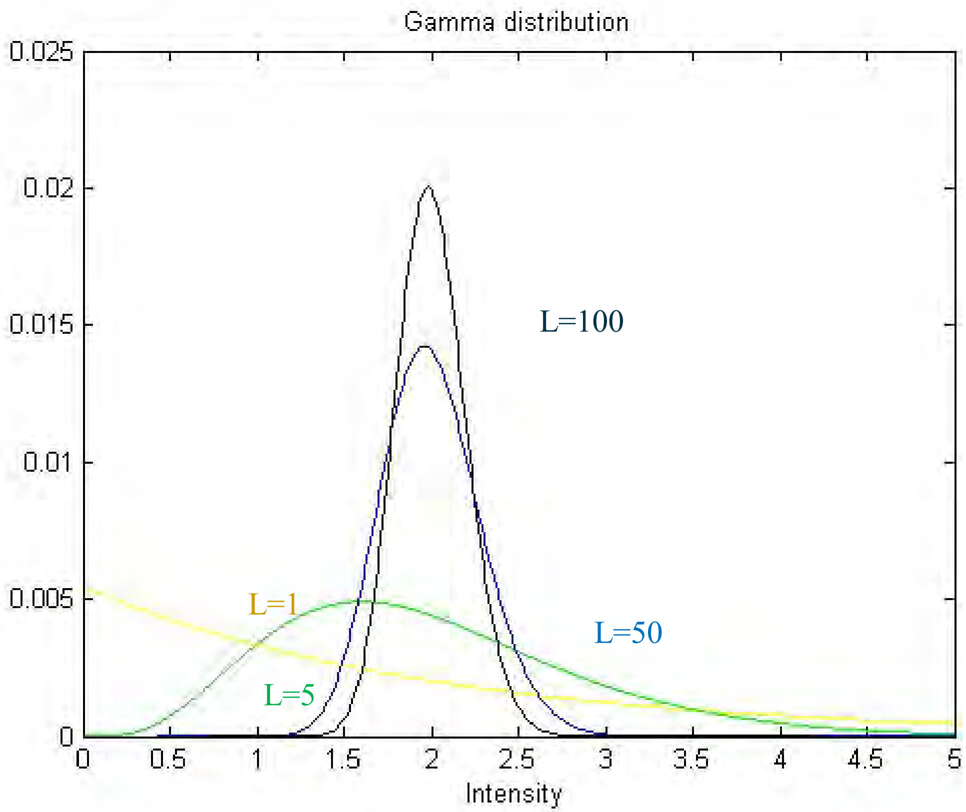

L =Equivalent Number of Looks

Main after averaging

$$\mu_L = E[I] = \tau$$

Variance after averaging

$$VAR_L = \frac{E[I]^2}{L} = \frac{\tau^2}{L}$$

The more we average the more the variance is reduced…
…always????

pdf for covariance matrix

If we assume Circular Complex Gaussian pixels the the covariance matrix is a Wishart

Wishart distribution (Covariance matrix):

$$[T] \sim W_c(p, n, \Sigma)$$

$$f_T(t) = \frac{1}{\Gamma_p(n)} \frac{1}{\Sigma^n} t^{n-p} \mathrm{e}^{-\mathrm{Trace}[\Sigma^{-1} t]}$$

$$\Gamma_p(n) = \pi^{p(p-1)/2} \prod_{j=1}^{p} \Gamma(n - j + 1)$$

Assumptions necessary for variance reduction

- ✓ The pixels averaged together has to be **independent** and come from the **same distribution** (independent and identically distributed iid).
- ✓ If more distributions are put together (e.g. we mix a road with forest) what comes out is neither one or another and can have a VARIANCE even higher than the original individual distribution.
- ✓ An example of dealing with heterogeneous targets are the **texture** pdf.
- ✓ When you average a textured area its variance does not reduce as the number of independent looks.

Texture: K distribution

pdf

$$f_K\left(k \mid \nu, E[k]\right) = \frac{2}{k}\left[\frac{L\nu k}{E[k]}\right]^{\frac{L+\nu}{2}} \frac{1}{\Gamma(\nu)\Gamma(L)} K_{\nu-L}\left[2\sqrt{\frac{L\nu k}{E[k]}}\right]$$

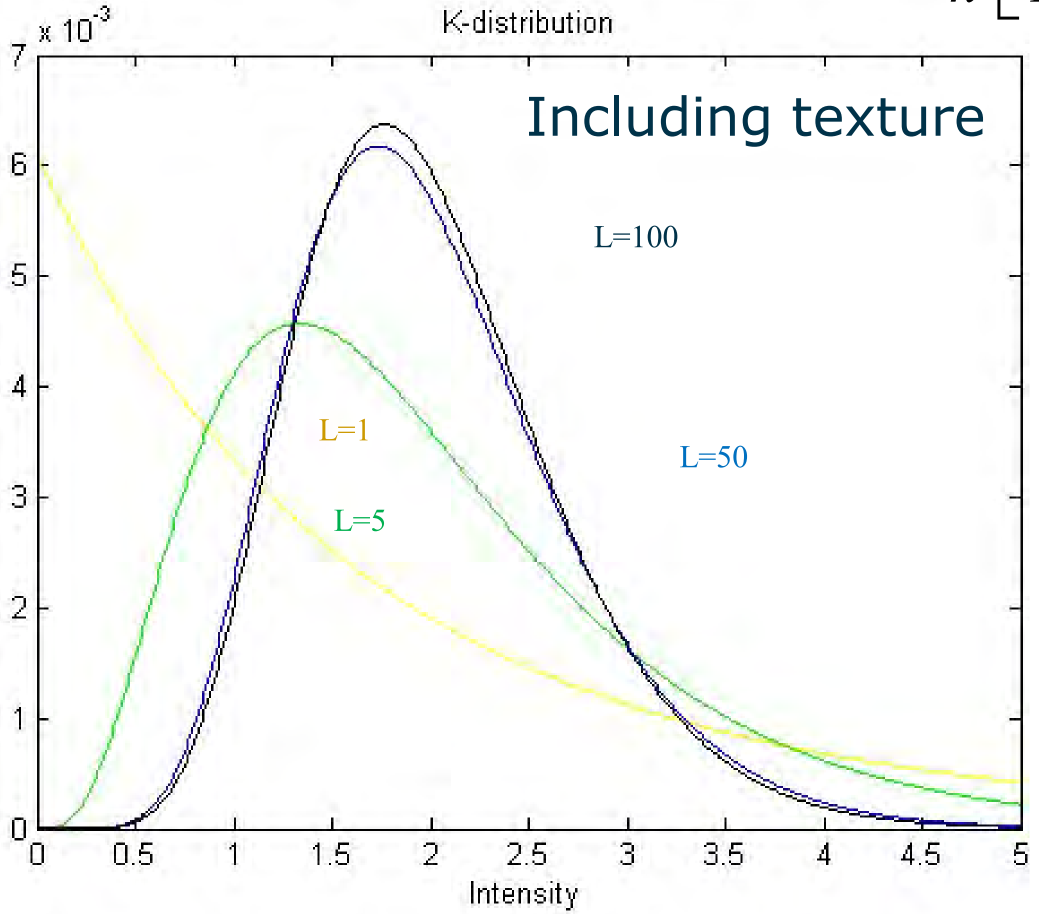

Including texture

$$\mu_L = E[k]$$

$$VAR_L = E[k]^2 \frac{\nu + L + 1}{\nu L}$$

- ✓ There are several distribution that can model the **texture** variations in the images.
- ✓ A complete treatment is outside the purpose of this presentation, here I show one of the models often used for the sea.

Independent looks??

- ✓ The L we see in the pdf equation is the **Equivalent Number of Looks ENL**.
- ✓ Pixels are not fully independent due to processes in image formation. Therefore, if you average 10 pixels your ENL is much lower than 10.
- ✓ There are tools for estimating the ENL, the simplest is based on the assumption of having an **homogeneous area with fully developed speckle**, i.e. the averaged intensity is a Gamma distribution.

$$ENL = \frac{E[x]^2}{VAR} = \frac{E[x]^2}{E\left[\left(x - E[x]\right)^2\right]}$$

- ✓ For a Gamma we know that $\mu_L = E[I] = \tau$ and $VAR_L = \frac{E[I]^2}{L} = \frac{\tau^2}{L}$
- ✓ Therefore, we the estimator for ENL is

$$ENL = \frac{\tau^2}{\tau^2} L = \mathrm{L}$$

Lee, J. S. & Pottier, E., Polarimetric radar imaging: from basics to applications, *CRC Press, Taylor & Francis Group*, **2009**

Corregistration

- ✓ One issue in change detection, is that the two images have to **overlap** perfectly.
  - ✓ Each pixel of each image has to be located at the same geographical point. If this is not true, we may detect changes just because we are looking at different areas.

- ✓ The process of making two images overlap is often called **Co-registration.**

Single-pol change detection: incoherent

If img_1 is one image acquired before the change (archive image) and img_2 is acquired after, we can use a “change detector”.

Change detector: an algorithm that detects “changes” between two images acquired at different moments in time.

Two very easy detectors can be devised considering the difference or the ratio of the intensities

$$\Delta I = \left| \left\langle |img_1|^2 \right\rangle - \left\langle |img_2|^2 \right\rangle \right| > T_1 \qquad \rho_I = \frac{\left\langle |img_1|^2 \right\rangle}{\left\langle |img_2|^2 \right\rangle} > T_2$$

The difference can also be normalised as

$$\Delta I_n = \frac{\left| \left\langle |img_1|^2 \right\rangle - \left\langle |img_2|^2 \right\rangle \right|}{\left\langle |img_1|^2 \right\rangle + \left\langle |img_2|^2 \right\rangle} > T_3$$

A) Wishart Change detector

We can approach the change detection as an hypothesis testing assuming the statistics of the covariance matrix are a Wishart distribution

$$[T_{11}] \sim W_c(p, n, [\Sigma_{11}]) \qquad [T_{22}] \sim W_c(p, m, [\Sigma_{22}])$$

p: number of polarimetric channels used
n: ENL for first acquisition
m: ENL for second acquisition
$[\Sigma_{11}]$: asymptotic covariance matrix of first acquisition
$[\Sigma_{22}]$: asymptotic covariance matrix of second acquisition

We can calculate the Likelihood Ratio test:

$$Q = \frac{(n+m)^{p(n+m)}}{n^{pn} m^{pm}} \frac{Det([T_{11}])^n Det([T_{22}])^m}{Det([T_{11}] + [T_{22}])^{n+m}}$$

Conradsen, K.; Nielsen, A. A.; Schou, J. & Skriver, H., A Test Statistic in the Complex Wishart Distribution and Its Application to Change Detection in Polarimetric SAR Data, *IEEE Trans. on Geos. & Rem. Sen.*, **2003**, *41*

B) Geometrical Perturbation Filter

- ✓ In order to work with partial target we first build a partial feature target starting from the covariance matrix

$$\underline{t}=\mathrm{Trace}([\mathrm{C}]\Psi) = [\langle|k_1|^2\rangle, \langle|k_2|^2\rangle, \langle|k_3|^2\rangle, \langle k_1^* k_2\rangle, \langle k_1^* k_3\rangle, \langle k_2^* k_3\rangle]^T$$

- ✓ In the data we can look for coherence between the target to be detected and a perturbed version of this.
  - ✓ If the coherence is high, it means that the target is present in the scene (because the projection of the pixels over that target and the perturbed one are correlated to each other).
  - ✓ If the coherence is low, we are looking at a part of the polarimetric space where there is no actual target.

$$\hat{\underline{t}}_T = \left[[T_T]_{11}, [T_T]_{22}, [T_T]_{33}, [T_T]_{12}, [T_T]_{13}, [T_T]_{23}\right]^T / \|\underline{t}_T\|$$: target to detect

$$\hat{\underline{t}}_P = \left[[T_P]_{11}, [T_P]_{22}, [T_P]_{33}, [T_P]_{12}, [T_P]_{13}, [T_P]_{23}\right]^T / \|\underline{t}_P\|$$: perturbed target

B) Geometrical Perturbation Filter

$$\underline{t}=\mathrm{Trace}([C]\Psi) = [\langle|k_1|^2\rangle, \langle|k_2|^2\rangle, \langle|k_3|^2\rangle, \langle k_1^* k_2\rangle, \langle k_1^* k_3\rangle, \langle k_2^* k_3\rangle]^T$$

$$\underline{\hat{t}}_T = [[T_T]_{11}, [T_T]_{22}, [T_T]_{33}, [T_T]_{12}, [T_T]_{13}, [T_T]_{23}]^T / \|\underline{t}_T\|$$

: target to detect

$$\underline{\hat{t}}_P = \left[[T_P]_{11}, [T_P]_{22}, [T_P]_{33}, [T_P]_{12}, [T_P]_{13}, [T_P]_{23}\right]^T / \|\underline{t}_P\|$$

: perturbed target

B) Geometrical Perturbation Filter

Based on a coherence → Independent on the overall amplitude

$$\gamma = \frac{\underline{\hat{t}}_T^{*T}\langle[P]\rangle\underline{\hat{t}}_P}{\sqrt{\underline{\hat{t}}_T^{*T}\langle[P]\rangle\underline{\hat{t}}_T\cdot\underline{\hat{t}}_P^{*T}\langle[P]\rangle\underline{\hat{t}}_P}}$$

$$P_{tot} = \langle \underline{t}^{*T}\cdot\underline{t}\rangle \qquad P_T = \left\langle \left|\underline{t}^{*T}\cdot\underline{\hat{t}}_T\right|^2\right\rangle$$

Total Power

$$\gamma = \frac{1}{\sqrt{1+RedR\left(\frac{\langle \underline{t}^{*T}\cdot\underline{t}\rangle}{\left\langle \left|\underline{t}^{*T}\cdot\underline{\hat{t}}_T\right|^2\right\rangle}-1\right)}} = \frac{1}{\sqrt{1+RedR\left(\frac{P_{tot}}{P_T}-1\right)}}$$

Gain factor

Power of target

Marino, A.; Cloude, S. R. & Woodhouse, I. H., Detecting Depolarized Targets using a New Geometrical Perturbation Filter, *IEEE Transactions on Geoscience and Remote Sensing*, **2012**, *50*, 3787-3799

B) Geometrical Perturbation Filter: change detector

✓ We want to detect the target $\underline{t}_1$ inside the second acquisition $\underline{t}_2$

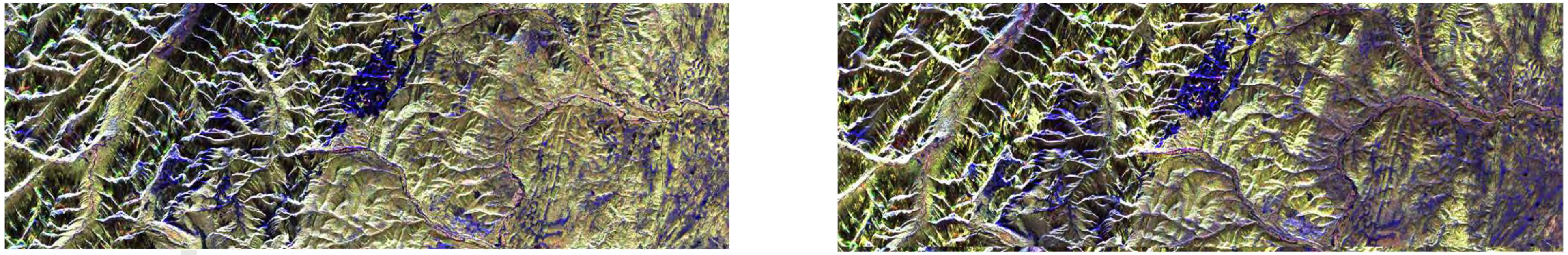

$$\hat{\underline{t}}_1 = \frac{\underline{t}_1}{\left\|\underline{t}_1\right\|}$$

$$\underline{t}_1(x,y)$$

$$\underline{t}_2(x,y)$$

$$\boxed{\gamma_d = \frac{1}{\sqrt{1+RedR\left(\frac{\left\langle \underline{t}_2^{*T}\cdot\underline{t}_2\right\rangle}{\left\langle \left|\underline{t}_2^{*T}\cdot\hat{\underline{t}}_1\right|^2\right\rangle}-1\right)}} \geq T}$$

$$\frac{1}{SCR} = \frac{\left\langle \underline{t}_2^{*T}\cdot\underline{t}_2\right\rangle}{\left\langle \left|\underline{t}_2^{*T}\cdot\hat{\underline{t}}_1\right|^2\right\rangle} - 1$$

Marino, A.; Cloude, S. R. & Lopez-Sanchez, J. M., A New Polarimetric Change Detector in Radar Imagery
IEEE Transactions on Gescience and Remote Sensing, **2013**, *51*, 2986 - 3000

ALOS quad pol

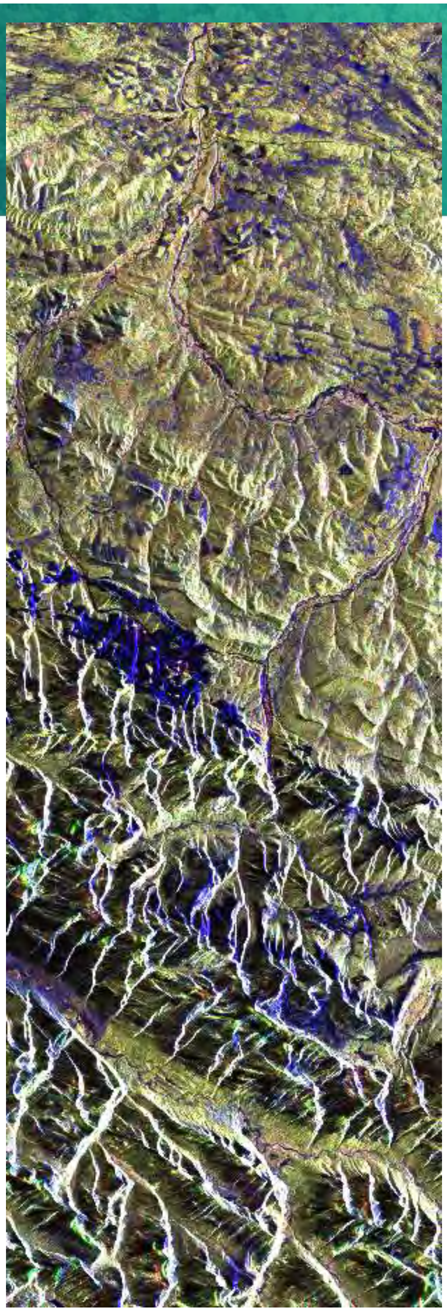

RGB1

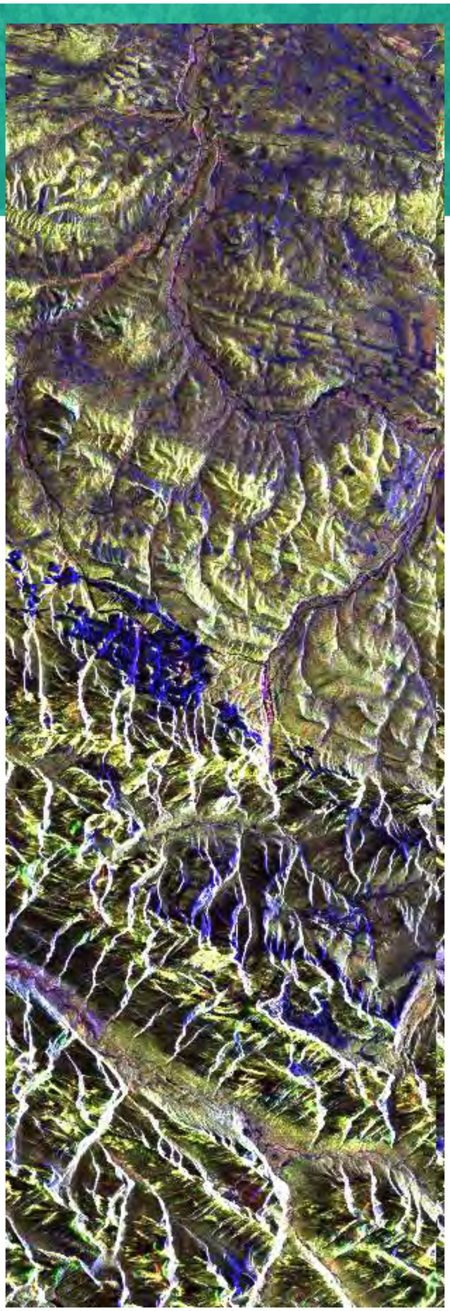

RGB2

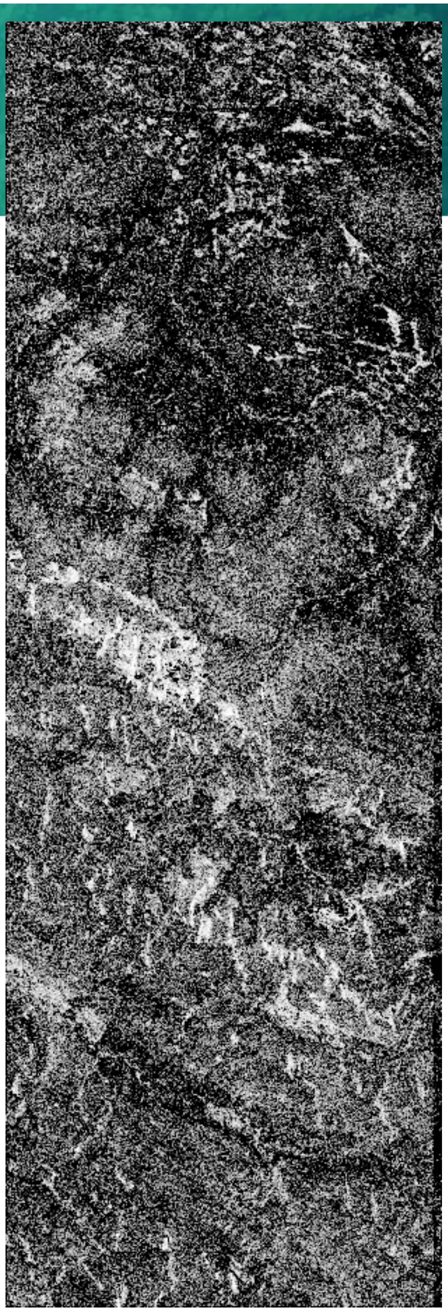

GPF $\Delta(\alpha / \beta) = 5$

Wishart 0.9

Data courtesy of Dr. Hao Chen
and Dr. David Goodenough,
Canadian Forestry Service
(CFS), Victoria, BC
JAXA©

C) Optimisations: power ratio

- ✓ Stemming from the idea of the PMF we can apply the filter to detect changes:

$$\rho_c = \frac{\underline{\omega}^{*T}[T_{11}]\underline{\omega}}{\underline{\omega}^{*T}[T_{22}]\underline{\omega}} = \frac{P_1}{P_2} \qquad [T_{22}]^{-1}[T_{11}]\underline{\omega} = \lambda\underline{\omega}$$

- ✓ Given two matrices $[T_{11}]$ and $[T_{22}]$ it is always possible to write $[T_{11}] = [A][T_{22}]$
  - ✓ Where [A] is a transformation matrix $[A] = [T_{11}][T_{22}]^{-1}$
- ✓ Since [T11] and [T22] are Hermitian, their inverse are Hermitian as well.

$$[A]^{*T} = \left([T_{11}][T_{22}]^{-1}\right)^{*T} = [T_{22}]^{-1}[T_{11}]$$

- ✓ The search space of this optimisation is the adjoint of the transformation that modify the partial target between the first and second acquisition
  - ✓ This transformation is **unique**, but it is not strictly a partial target.

Marino, A. & Hajnsek, I., A Change Detector Based on an Optimization With Polarimetric SAR Imagery, *IEEE Transactions on Geoscience and Remote Sensing*, **2014**, *52*, 4781-4798

d) Optimisations: power difference

- ✓ The power difference of scattering mechanisms (SM) composing two partial targets at two instant in time can be expressed as

$$\Delta = \underline{\omega}^{*T}\left[T_{22}\right]\underline{\omega} - \underline{\omega}^{*T}\left[T_{11}\right]\underline{\omega} \quad \Longrightarrow \quad \Delta = \underline{\omega}^{*T}([T_{22}] - [T_{11}])\underline{\omega} = \underline{\omega}^{*T}[T_c]\underline{\omega}$$

$$L = \underline{\omega}^{*T}[T_c]\underline{\omega} - \lambda\left(\underline{\omega}^{*T}\underline{\omega} - Const\right) \quad \Longrightarrow \quad \frac{\partial L}{\partial \underline{\omega}^{*T}} = [T_c]\underline{\omega} - \lambda\underline{\omega} \quad \Longrightarrow \quad [T_c]\underline{\omega} = \lambda\underline{\omega}$$

- ✓ We are interested in the **change matrix** $[T_c]=[T_{22}]-[T_{11}]$

- ✓ $[T_c]$ **has upper and lower triangular parts symmetric, it is Normal, but it is not positive semi-definite, so it is not Hermitian**

- ✓ It represents the combination of SMs with positive or negative power. This is because a SM that reduce its power will be seen as having a negative power.

Marino, A., & Alonso-Gonzalez, A. An optimization of the difference of covariance matrices for PolSAR change detection, IGARSS 2017.

d) Optimisations: signal models

Before | After

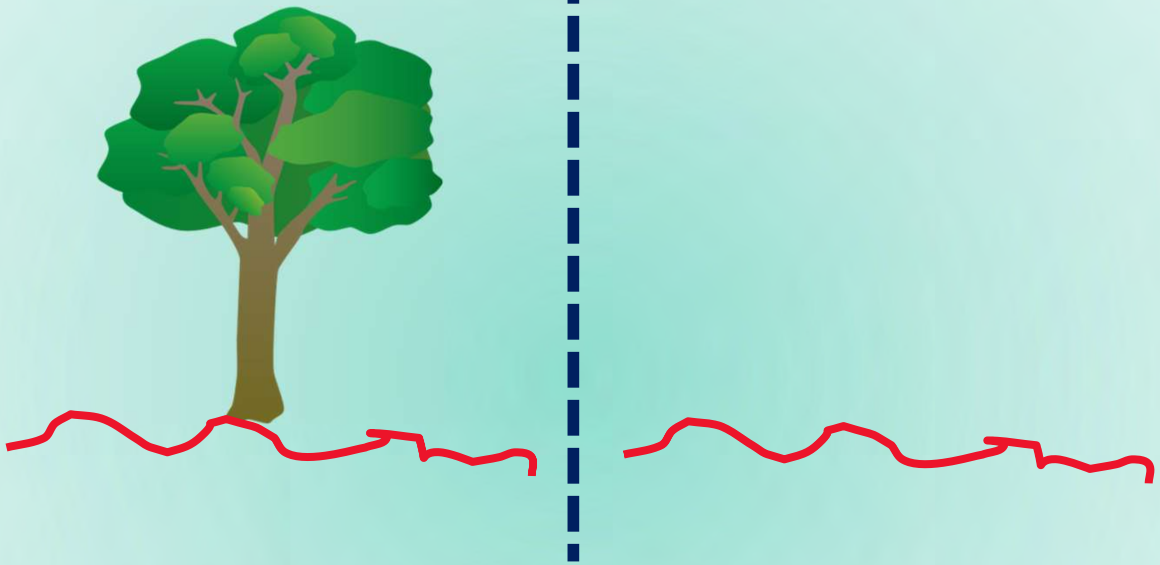

Additive model: when a change is produced by adding or subtraction a target. Change detectors are generally obtained considering differences.

Before | After

Multiplicative model: when a change is produced by transforming the target. If we still assume linearity this transformation is done multiplying by a matrix.

ALOS quad-pol: Morecambe Bay

Tidal area,
Morecambe Bay, UK
2007 JAXA©

1 April 2007

RGB image: First

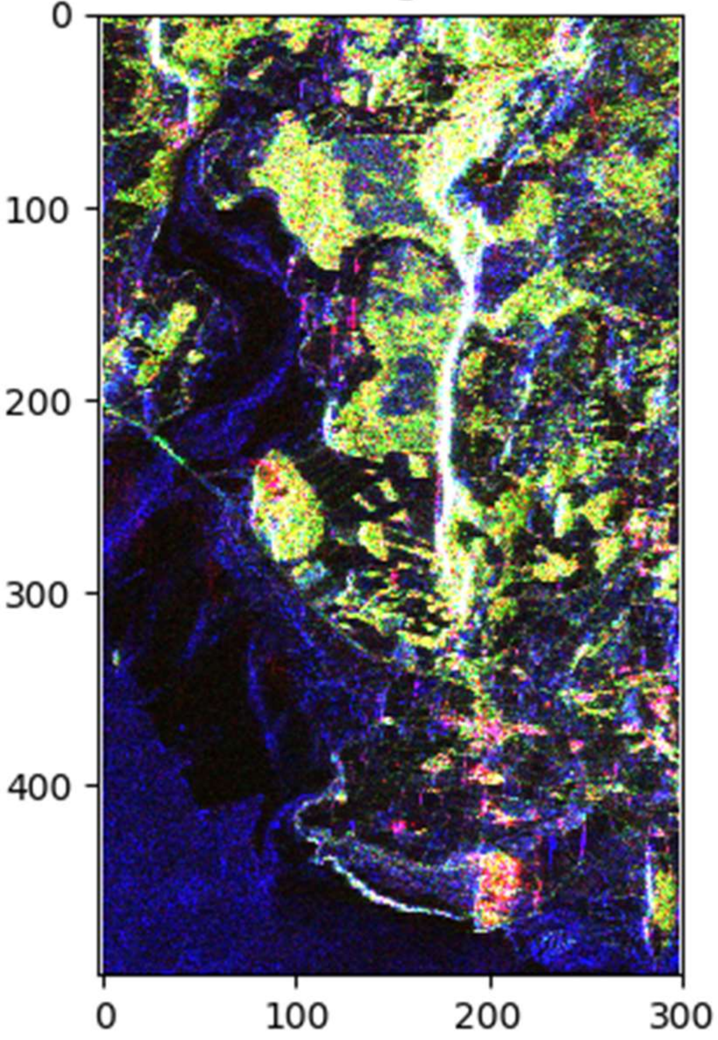

17 May 2007

RGB image: Second

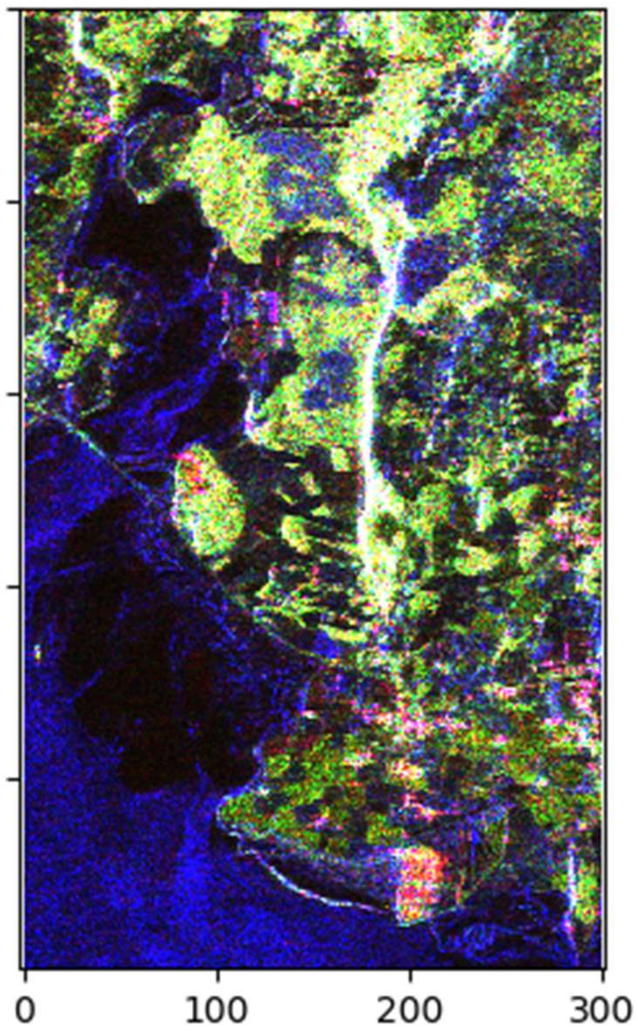

c) Morecambe Bay: mult. RGB composite

$$[T_{22}]^{-1}[T_{11}]\underline{\omega} = \lambda\underline{\omega}$$

- ✓ The value of the RGB is modulated by the eigenvalue as in a Pauli basis RGB image
- ✓ The colour do NOT seems to correspond to excepted SM
- ✓ The detector is able to identify changes as for erosion

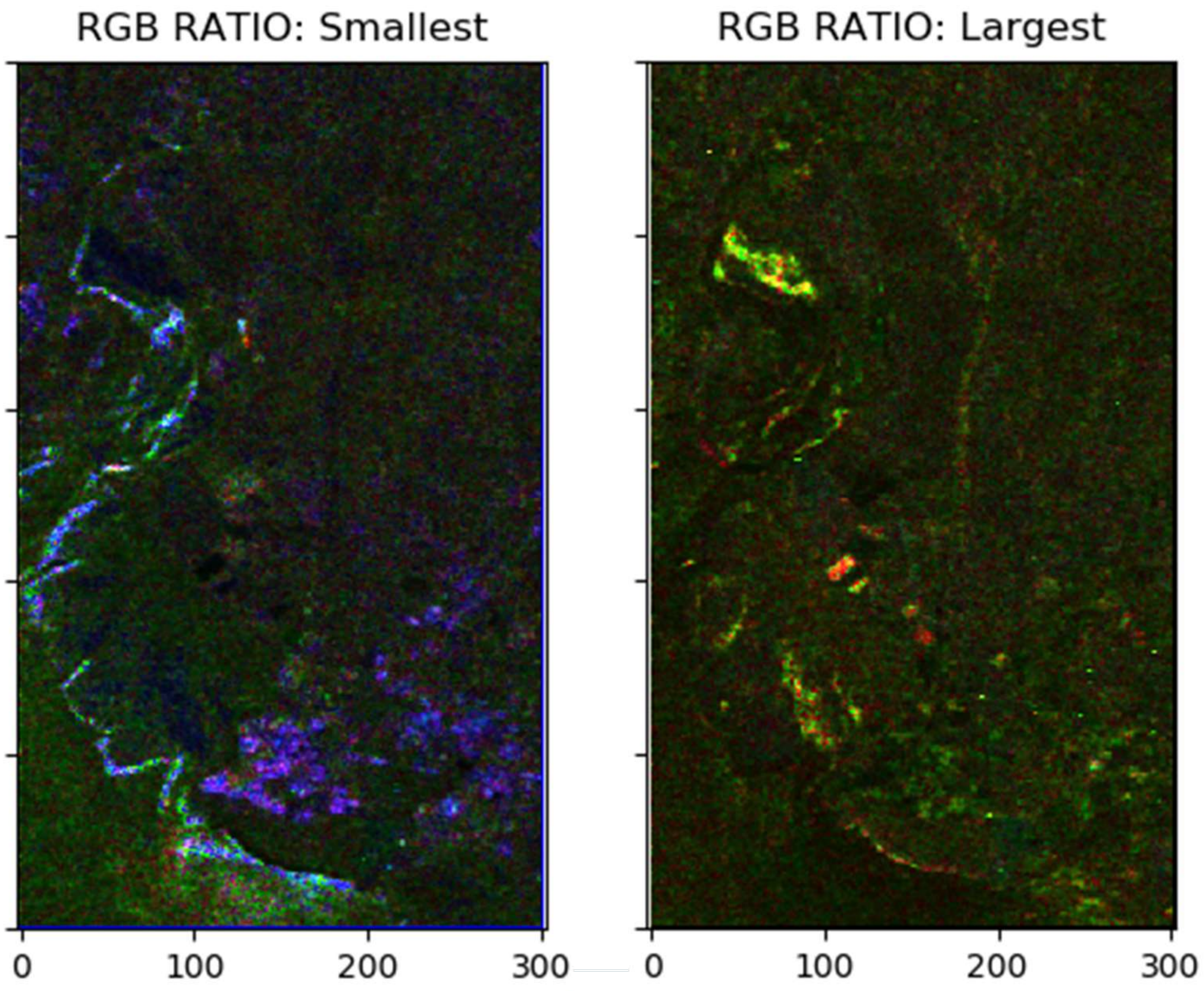

d) Morecambe Bay: additive RGB composite

$$([T_{22}] - [T_{11}])\underline{\omega} = \lambda\underline{\omega}$$

- ✓ The value of the RGB is modulated by the eigenvalue as in a Pauli basis RGB image
- ✓ The colour do seems to correspond to excepted SM (e.g. changes in power of surface scattering over the sea, or volume over the agricultural fields)

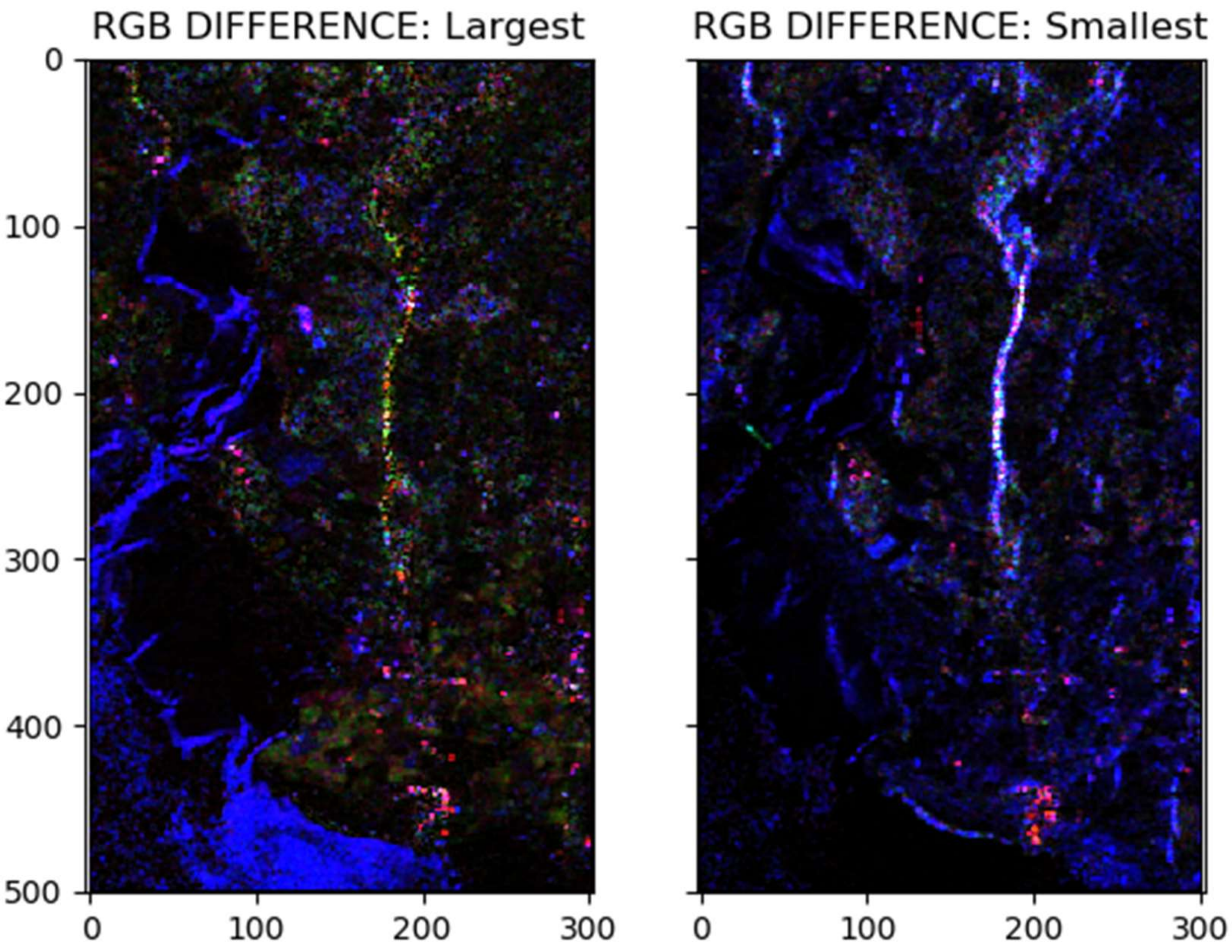

Agriculture: Time series

Using time information

- ✓ Imagine we only have a single snapshot to look at the scene…
- ✓ It is sometimes hard to know what is going on there.

https://www.thecomicstrips.com/subject/The-Misunderstand-Comic-Strips-by-Mike+du+Jour.php

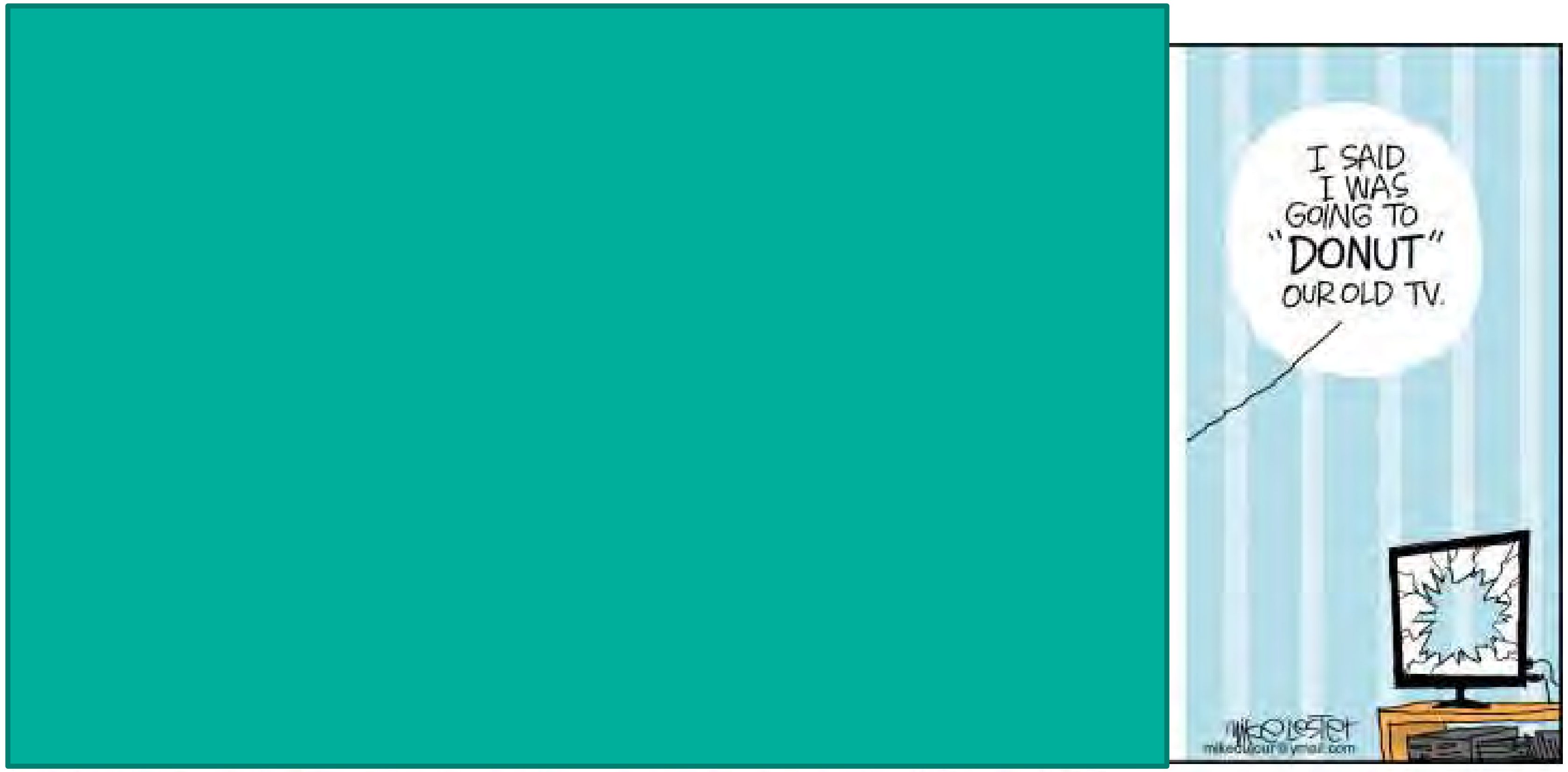

©Mike Lester

Using time information

- ✓ Imagine we only have a single snapshot to look at the scene…
- ✓ It is something hard to know what is going on there.
- ✓ But if we add the temporal information ambiguities are much easier to disentangle

https://www.thecomicstrips.com/subject/The-Misunderstand-Comic-Strips-by-Mike+du+Jour.php

PolSAR-App experiment

- ✓ This is particularly beneficial for monitoring very **dynamic systems** as agriculture
- ✓ One “direct” way is to prepare **time series** of polarimetric parameters/observables and look at how they evolve in time
- ✓ In PolSAR-App a test was done using RADARSAT-2 AgriSAR2009 images

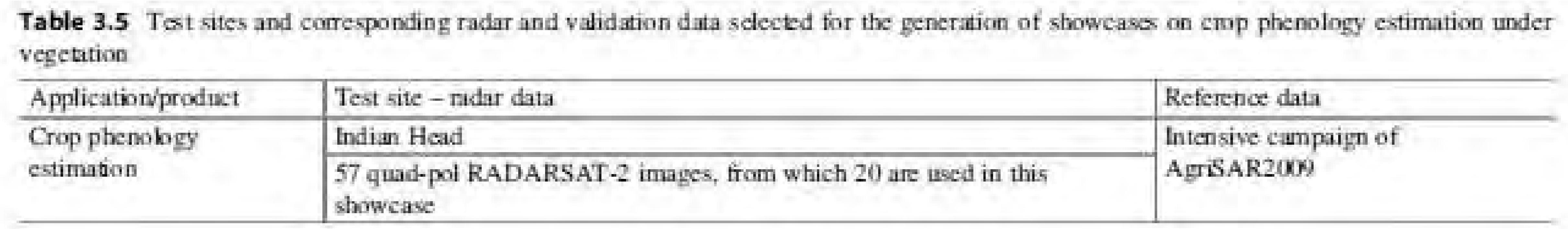

Table 3.5 Test sites and corresponding radar and validation data selected for the generation of showcases on crop phenology estimation under vegetation

Application/product	Test site – radar data	Reference data
Crop phenology estimation	Indian Head	Intensive campaign of AgriSAR2009
	57 quad-pol RADARSAT-2 images, from which 20 are used in this showcase	

Time series

- ✓ Different fields can show different trends
- ✓ Here we want to see if the trend can be used to classify the **phenological stage**
- ✓ In this case we look at cereals that are particularly different to separate from each other

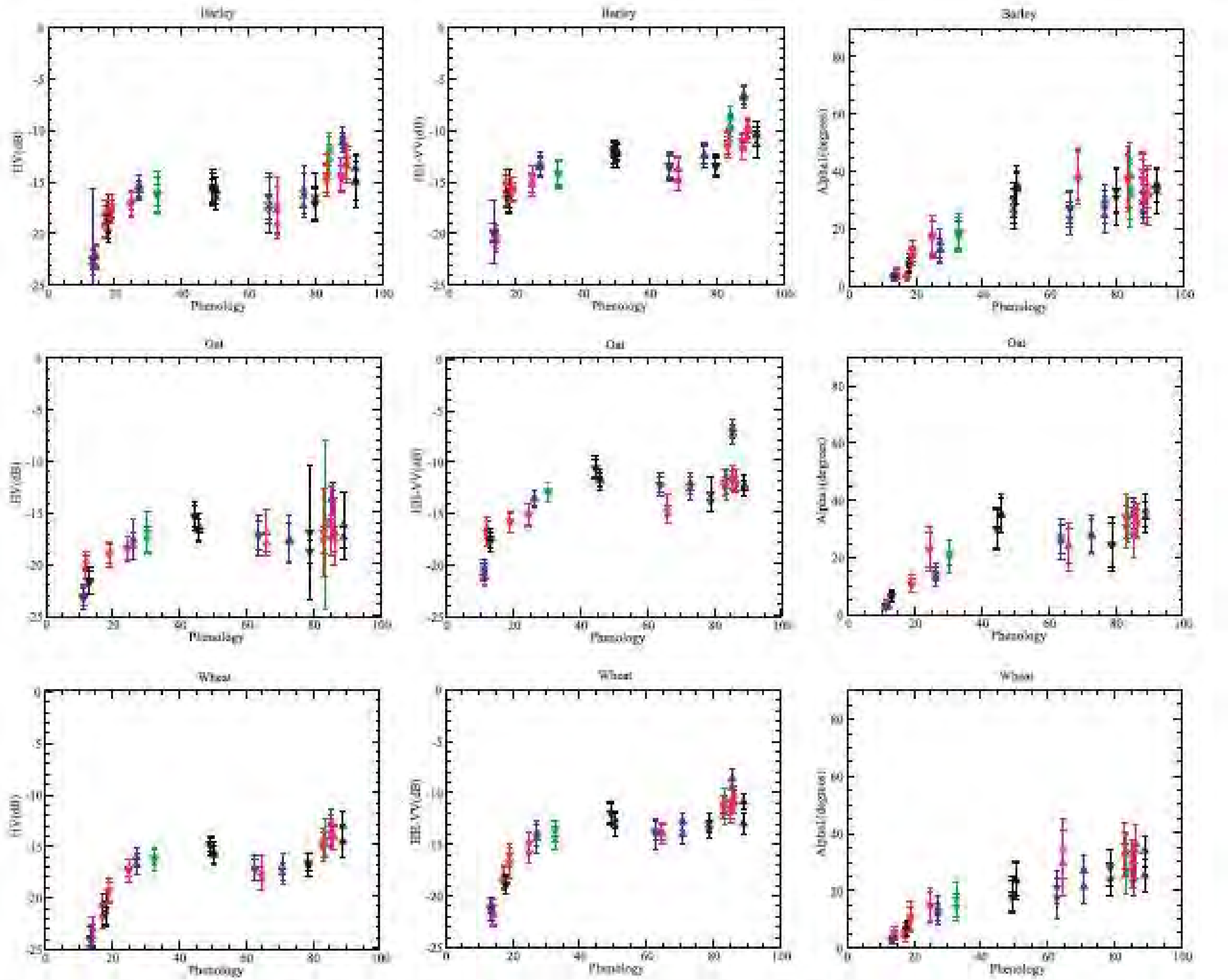

Fig. 3.14 Evolution of HV (t_{33}), HH – VV (t_{22}) and dominant alpha (α_1) as a function of phenology for barley (top row), oat (middle row) and wheat (bottom row)

Classification

- ✓ We can feed these trends to **adaptive filters** and **machine learning** methods to perform supervised classification.
- ✓ This allows to identify in which phenological stage the crop is.

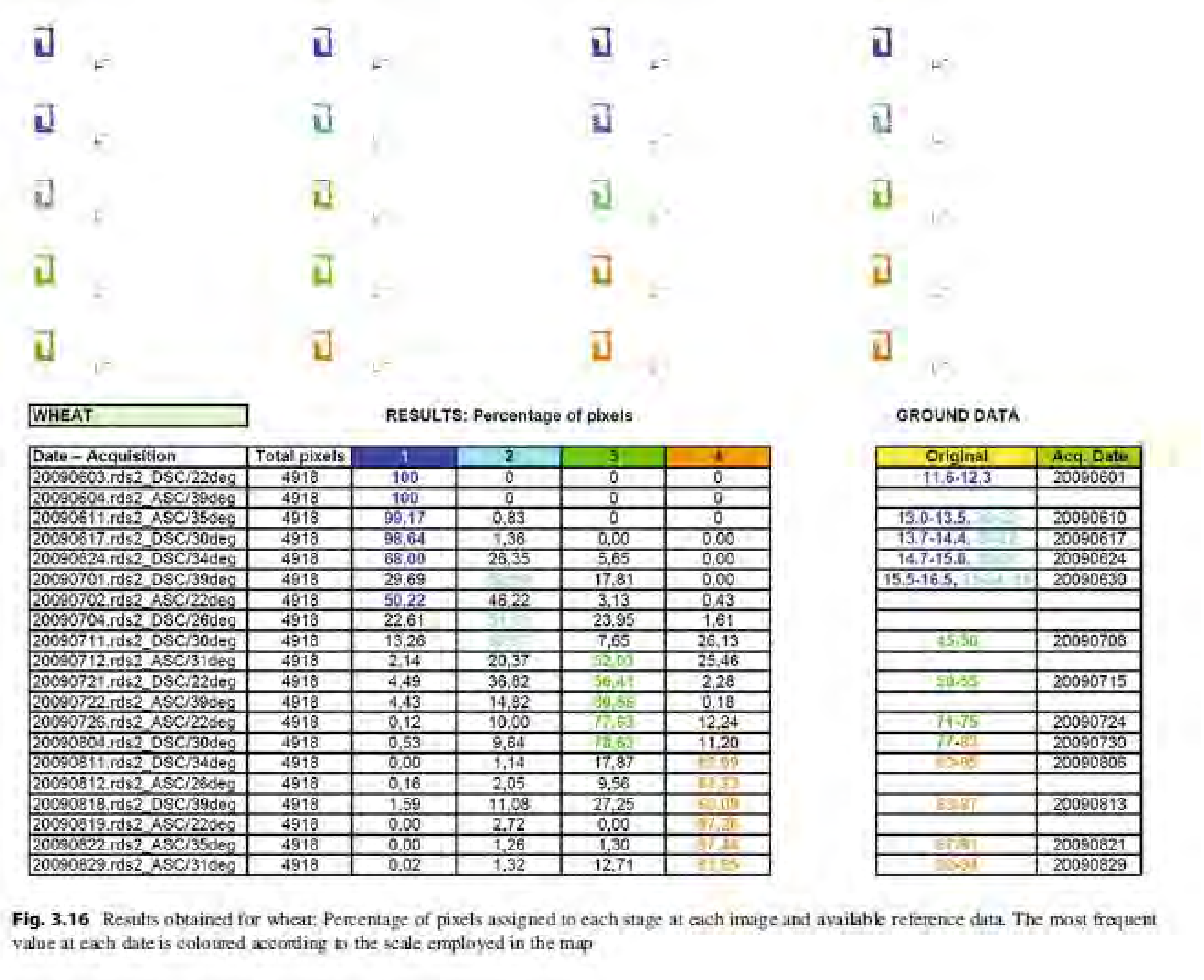

WHEAT

RESULTS: Percentage of pixels

Date – Acquisition	Total pixels	1	2	3	4
20090603.rds2_DSC/22deg	4918	100	0	0	0
20090604.rds2_ASC/39deg	4918	100	0	0	0
20090611.rds2_ASC/35deg	4918	99,17	0,83	0	0
20090617.rds2_DSC/30deg	4918	98,64	1,36	0,00	0,00
20090624.rds2_DSC/34deg	4918	68,00	26,35	5,65	0,00
20090701.rds2_DSC/39deg	4918	29,69	52,50	17,81	0,00
20090702.rds2_ASC/22deg	4918	50,22	46,22	3,13	0,43
20090704.rds2_DSC/26deg	4918	22,61	51,83	23,95	1,61
20090711.rds2_DSC/30deg	4918	13,26	52,96	7,65	26,13
20090712.rds2_ASC/31deg	4918	2,14	20,37	52,03	25,46
20090721.rds2_DSC/22deg	4918	4,49	36,82	56,41	2,28
20090722.rds2_ASC/39deg	4918	4,43	14,82	59,56	0.18
20090726.rds2_ASC/22deg	4918	0,12	10,00	77,63	12,24
20090804.rds2_DSC/30deg	4918	0,53	9,64	78,63	11,20
20090811.rds2_DSC/34deg	4918	0,00	1,14	17,87	80,99
20090812.rds2_ASC/26deg	4918	0,16	2,05	9,56	88,23
20090818.rds2_DSC/39deg	4918	1.59	11,08	27,25	60,09
20090819.rds2_ASC/22deg	4918	0,00	2,72	0,00	97,28
20090822.rds2_ASC/35deg	4918	0,00	1,26	1,30	97,44
20090829.rds2_ASC/31deg	4918	0,02	1,32	12,71	85,95

GROUND DATA

Original	Acq. Date
11.6-12.3	20090601
13.0-13.5, [illegible]	20090610
13.7-14.4, [illegible]	20090617
14.7-15.6, [illegible]	20090624
15.5-16.5, [illegible]	20090630
45-50	20090708
50-55	20090715
71-75	20090724
77-83	20090730
83-85	20090806
83-87	20090813
87-91	20090821
90-94	20090829

Fig. 3.16 Results obtained for wheat: Percentage of pixels assigned to each stage at each image and available reference data. The most frequent value at each date is coloured according to the scale employed in the map

Comparison

- ✓ The table show useful polarimetric observables for monitoring the phenological stage
- ✓ A comparison was also done with different polarimetric mode showing that full poll could improve the classification in some conditions.

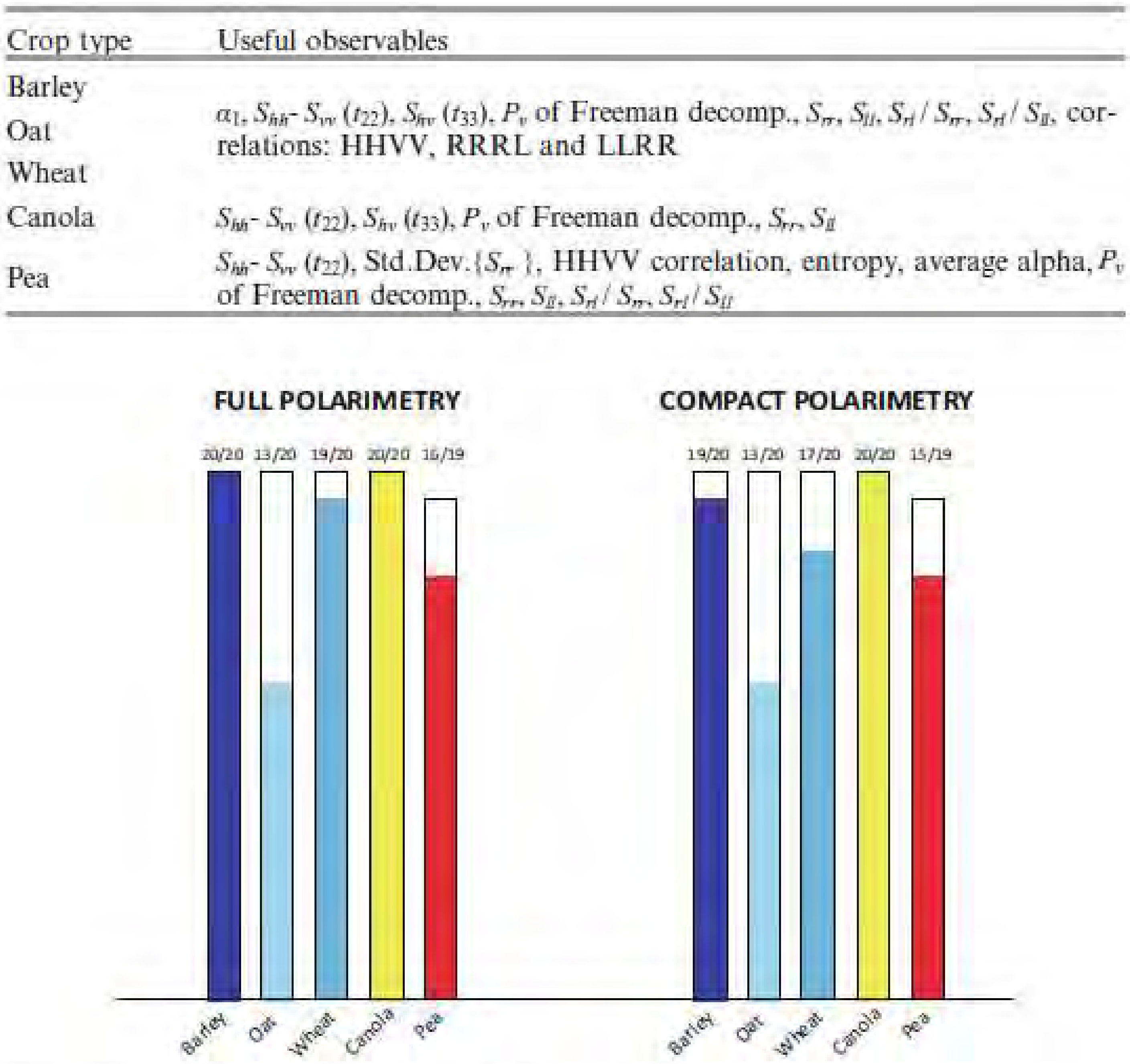

Crop type	Useful observables
Barley	α_1, S_{hh}- S_{vv} (t_{22}), S_{hv} (t_{33}), P_v of Freeman decomp., S_{rr}, S_{ll}, S_{rl} / S_{rr}, S_{rl} / S_{ll}, correlations: HHVV, RRRL and LLRR
Oat	
Wheat	
Canola	S_{hh}- S_{vv} (t_{22}), S_{hv} (t_{33}), P_v of Freeman decomp., S_{rr}, S_{ll}
Pea	S_{hh}- S_{vv} (t_{22}), Std.Dev.{S_{rr} }, HHVV correlation, entropy, average alpha, P_v of Freeman decomp., S_{rr}, S_{ll}, S_{rl} / S_{rr}, S_{rl} / S_{ll}

Fig. 3.17 Top: summary of useful parameters for each crop type. Bottom: overall performance

Thank you very much for your attention.

Senior Lecturer in Earth observation,
Biological and Environmental Sciences
University of Stirling
FK9 4LA | Stirling | UK
T +44 (0) 1786 66565
Earmando.marino@stir.ac.uk